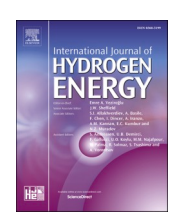
ELSEVIER

Contents lists available at ScienceDirect

International Journal of Hydrogen Energy

journal homepage: www.elsevier.com/locate/he





Enabling industrial decarbonization: A MILP optimization model for low-carbon hydrogen supply chains

Jan L. Dautel^a, Jagruti Thakur^{a,*}, Ahmed M. Elberry^{b,c}

- ^a Department of Energy Technology, KTH Royal Institute of Technology, Stockholm, Sweden
- ^b Faculty of Science (HIMS), University of Amsterdam, Amsterdam, the Netherlands
- ^c TNO Energy and Materials Transition, Amsterdam, the Netherlands

ARTICLE INFO

Handling Editor: Ibrahim Dincer

Keywords:
Hydrogen supply chain
Optimization
LCOH
Renewable energy
Industry

ABSTRACT

This study develops a an optimization model focused on the layout and dispatch of a low-carbon hydrogen supply chain. The objective is to identify the lowest Levelized Cost of Hydrogen for a given demand. The model considers various elements, including electricity supply from the local grid and renewable sources (photovoltaic and wind), alongside hydrogen production, compression, storage, and transportation to end users. Applied to an industrial case study in Sweden, the findings indicate that the major cost components are linked to electricity generation and investment in electrolyzers, with the LCOH reaching 5.2 EUR/kgH2 under typical demand conditions. Under scenarios with higher peak demands and greater demand volatility, the LCOH increases to 6.8 EUR/kgH2 due to the need for additional renewable energy capacity. These results highlight the critical impact of electricity availability and demand fluctuations on the LCOH, emphasizing the complex interdependencies within the hydrogen supply chain. This study provides valuable insights into the feasibility and cost-effectiveness of adopting hydrogen as an energy carrier for renewable electricity in the context of decarbonizing industrial processes in the energy system.

Abbreviation

GHI	Global Horizontal Irradiance
LCOH	Levelized Cost of Hydrogen
MILP	Mixed-Integer Linear Optimization Problem
NPC	Net Present Cost
PEM	Proton Exchange Membrane
PoA	Plane of Array
PV	Photovoltaic
RE	Renewable Energy
STP	Standard Temperature and Pressure

1. Introduction

In the wake of growing environmental concerns and the global push towards decarbonization, the industrial sector stands at a crossroads. Among the various challenges they face, reducing greenhouse gas emissions while maintaining economic growth remains a paramount goal. This in turn places the transformation of energy systems at the forefront of global sustainability efforts. To this end, the adoption of

renewable energy, energy efficiency measures, and low-carbon technologies represent critical strategies for creating a more sustainable and self-sufficient energy system [1]. Together, these elements form the cornerstone of a sustainable energy future.

Hydrogen, with its unique properties, stands out as a promising solution in this new energy landscape. It offers a path to decarbonize sectors where electrification poses challenges, such as in high-temperature industrial processes prevalent in steel, cement, and chemical production [2]. The potential of hydrogen to be produced from renewable electricity through the process of electrolysis further underscores its role in industrial sustainability [3]. Numerous research studies have investigated diverse approaches to hydrogen production, encompassing methods involving fossil fuels, such as coal gasification and steam reforming, as well as electricity-based processes, such as water electrolysis and thermolysis [4–8]. The logistics of supplying hydrogen, encompassing storage and transport, also present a diverse technical and economic challenges, as explored in Refs. [9–11].

While technical barriers to hydrogen adoption are not significant, with many key technologies already mature, the landscape is still fraught with regulatory and economic uncertainties [12]. The

E-mail address: jrthakur@kth.se (J. Thakur).

https://doi.org/10.1016/j.ijhydene.2024.06.050

^{*} Corresponding author.

complexity of hydrogen's role in an interconnected energy system is often overlooked, especially when considering the full spectrum of its production, storage, transportation, and utilization. Such complexity demands a nuanced understanding that extends beyond individual components. In their respective studies, Elberry et al. [13] and Mintz et al. [14], assert that the determination of the most feasible hydrogen storage type and its optimal scale is closely tied to the specificities of individual cases. This underscores the imperative of considering the entire supply chain in such evaluations, revealing an inherent interdependence. Numerous studies have successfully investigated the design of hydrogen supply chain networks by utilizing a linear programming approach with various scopes and objectives, while only few consider the total supply chain cost and the discounting of future cash flows [15]. Hence, due to the identified research gaps, these studies [16,17] highlight that the optimization models focusing on the future design of hydrogen supply chain needs to be evaluated, however, only considering fuelling infrastructure on national level. Expanding this scope to multiple use cases for hydrogen, Husarek et al. [18] describe a linear programming optimization model for a predicted hydrogen demand for Germany in 2050, considering multiple production and transport options and potential import and export of hydrogen. Further, to address the arising challenge of prediction uncertainty, Nunes et al. [19] as well as Erdogan and Gueler [20] introduce optimization approaches under uncertain demand development on national level. Similarly, the work of Brändle et al. [21] propose a system optimization for a hydrogen production chain on national level. However, they omit considerations related to the dynamic short- and long-term intermittency of supply and demand. Riera et al. [22] reviewed recent literature of hydrogen production and supply chain modelling and optimization, concluding that coarse time resolution results in suboptimal system designs as potential correlation between intermittent resource availability and hydrogen demand cannot be captured. They emphasize the need for models with high temporal resolution. Considering a day-to-day variability of feedstock availability and hydrogen demand, Almaraz et al. [23] proposed a model design for a hydrogen supply chain. While a daily resolution will be able to reflect seasonal variability, short term fluctuations of renewable energy (RE) is not captured. Addressing this gap, Yang et al. [11] and Gallardo et al. [24] utilize linear optimization models to assess the least-cost hydrogen supply for off-grid wind and solar photovoltaic (PV) systems, respectively, using hourly load profiles. Also, their models do not consider the intermittency of hydrogen demand and the possibility of grid connected hydrogen production. In the study of Seo et al. [25], an hourly resolution for supply and demand are chosen. However, they focus specifically on the design and impact of hydrogen storage options within the supply chain for fuel cell electric vehicle fuelling stations.

In terms of storage, Reuss et al. [26] propose an optimization model specifically focused on investigating various storage options, seeking to minimize costs across the entire supply chain from production to transport. However, the reliance on annual values in this model introduces considerations about the long-term dynamics of RE availability and hydrogen demand while potentially overlooking short-term impacts. Chen et al. [27] extend this exploration by focusing on hydrogen transport as liquified hydrogen, incorporating daily variability but not the seasonal shifts that significantly impact demand and RE generation.

This research seeks to bridge these gaps by proposing a comprehensive techno-economic analysis of the Levelized Cost of Hydrogen (LCOH). It considers the intermittency of electricity supplied from both the grid and RE sources with a detailed temporal resolution of 1 h, focusing on regional hydrogen production and consumption. By employing a linear optimization methodology, the analysis spans all phases of the supply chain, encompassing electricity procurement and/ or generation from intermittent RE sources, hydrogen production, storage, and eventual transport to end consumers (see Fig. 1). The primary objective is to determine the lowest LCOH, with regard to the layout and dispatch. An industrial case study situated in northern Sweden serves as the proving ground to ascertain the most economical supply chain configuration and to determine the optimal capacities and dispatch schedules under various demand scenarios on a detailed level. Through this exploration, we aim to enhance transparency and comprehension regarding the utilization of hydrogen as a low-carbon energy carrier.

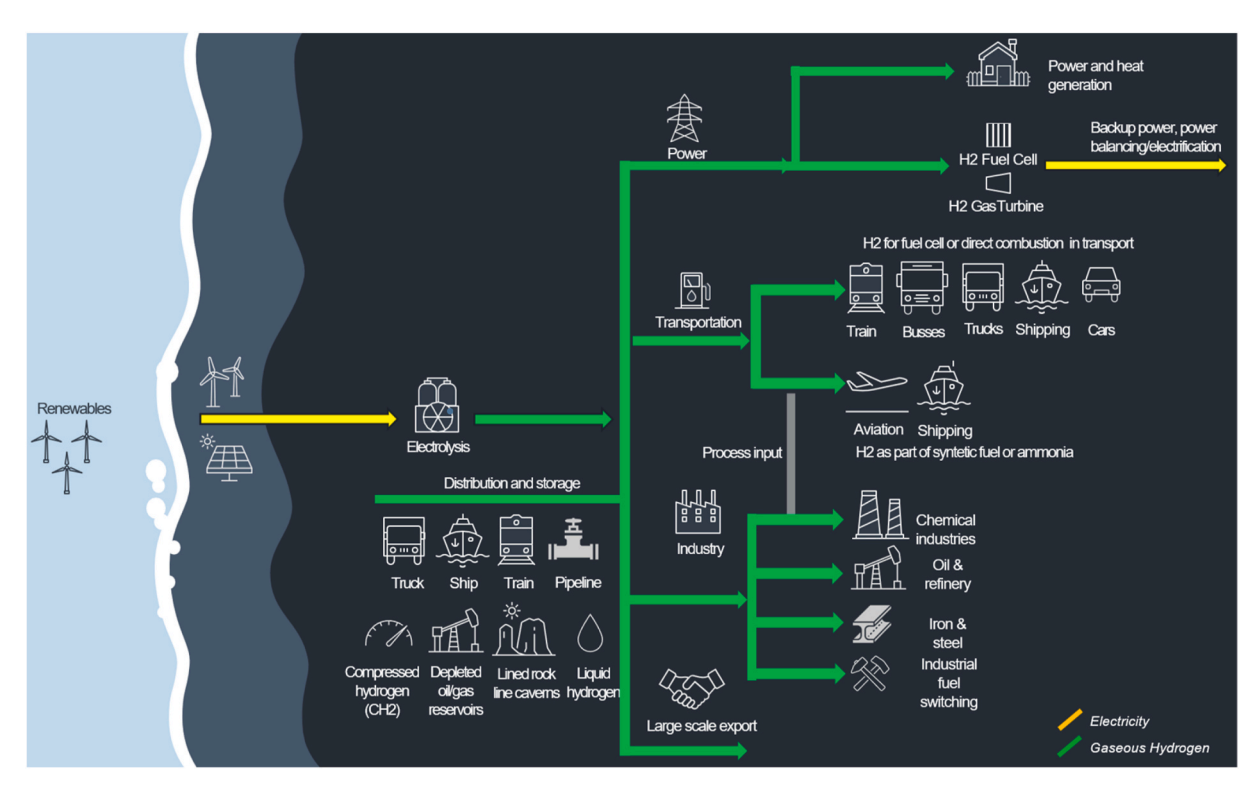


Fig. 1. Illustration of a hydrogen supply chain network.

The developed methodology and tool presented herein provide a versatile framework that is replicable, scalable, and can be adapted to diverse cases. The research thus contributes to the academic discourse by offering novel insights and a practical tool for the assessment of low-carbon hydrogen supply chains.

The remainder of this article is divided into five main sections as follows: Section 2, "Methods", describes the methodology used to design and analyse the proposed hydrogen supply chain model. This includes details on the utilized tools and the modelling approach. Section 3, "Case Study", introduces the industrial showcase and its corresponding data. Section 4, "Results", presents the results of the analysis, including the optimal hydrogen supply chain layout and the associated costs. Section 5, "Discussion", presents the implications of the results. The sixth and final section "Conclusion", summarizes the key findings of the study and their potential impact on the establishment of an economically viable hydrogen supply chain.

2. Methods

This section focusses on the designed method, in which the decision variables, the objective function, the technology specific parameters and constraints of all supply chain stages, along with the case specific data are introduced. Finally, a sensitivity analysis is conducted to highlight the impact of selected parameters.

The scope of the model consists of the layout and dispatch optimization of defined hydrogen demand cases as shown in Fig. 2. Electricity is considered as primary energy to produce hydrogen. RE sources such as on- and offshore wind power, and solar PV as well as the local grid can be utilized depending on the configuration of the model. The model can be used to investigate either a single option or determine the optimum share between multiple options. The RE can be utilized, stored in batteries, and curtailed, but no electricity is sold to the grid within the optimization model. Thus, RE sources are primarily dedicated to the production of hydrogen. However, the potential for generating additional revenue by selling surplus electricity to the electricity market is discussed as a future opportunity. In the model, water electrolysis is the method considered to produce hydrogen. Also, hydrogen is only considered to be in its gaseous form and transported on-land, however, further conversion into other forms such as liquified hydrogen or ammonia can be added in further research. Electrolyzer and hydrogen

storage are assumed to be collocated, meaning that the transport distance for hydrogen refers to the distance between storage and consumption unit. The most important inputs to the model are wind speeds, solar irradiation, air temperature, electricity price, hydrogen demand with hourly resolution. In addition, cost, and performance data for all the technologies is considered. The main outputs of the model will include optimum layout (installed capacities of all supply chain stages), optimum dispatch (hourly operational schedule), visualization of the energy flows and patterns and finally economic cost calculation.

The supply chain under investigation comprises four main stages: I) electricity generation and storage; II) hydrogen production; III) hydrogen compression and storage; IV) hydrogen transportation to the end consumer (see Fig. 2).

This study presents a comprehensive optimization modelling tool which is flexible and replicable for any location, various demands, as well as time resolution which can be specified by the user in the model and adjusted depending on the application. To compare relevant scenarios for every case, the user simply adjust the parameters that define the boundary conditions of the supply chain in the input file, which is EXCEL based. The defined parameters are used to build the Mixed-Integer Linear Optimization Problem (MILP) model which is constructed using the Pyomo-Library, a set of open-source Python software packages designed for developing optimization models in Python [28]. Finally, the computed results are post-processed in EXCEL, where the data is visualized, and statistical patterns are analyzed. Fig. 3 illustrates the sequential flow of the model.

2.1. Input file

The EXCEL based Input File is the user interface in which the boundary conditions of the model are set. Depending on the users' access to technology-specific data, the parameters can be adjusted to different levels of detail. By default, a set of parameters for each selectable technology is predefined but can be adjusted if more accurate or case specific data is available. Fig. 4 shows an overview of the structure of the Input File.

Within the system sheet, the following boundary conditions of the optimization problem are set. An overview of the SYSTEM-Sheet can be found in Appendix A. Here, the main adjustable boundary conditions are as follows:

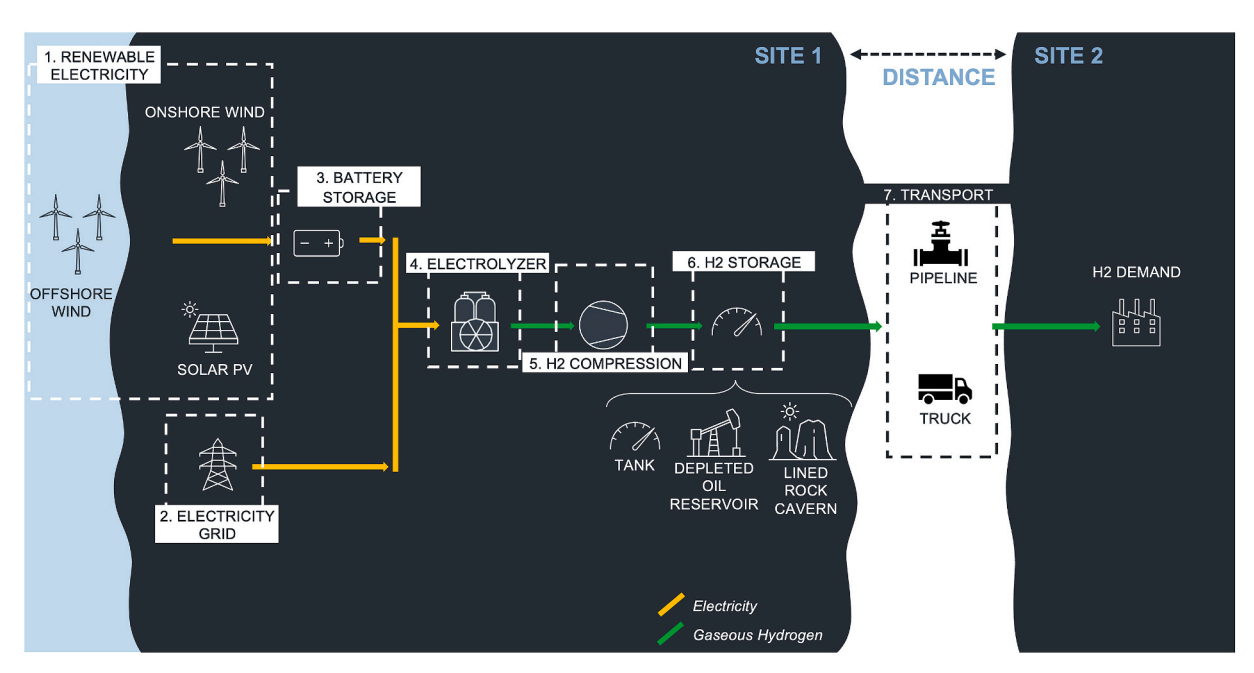


Fig. 2. Illustration of the considered hydrogen supply chain.

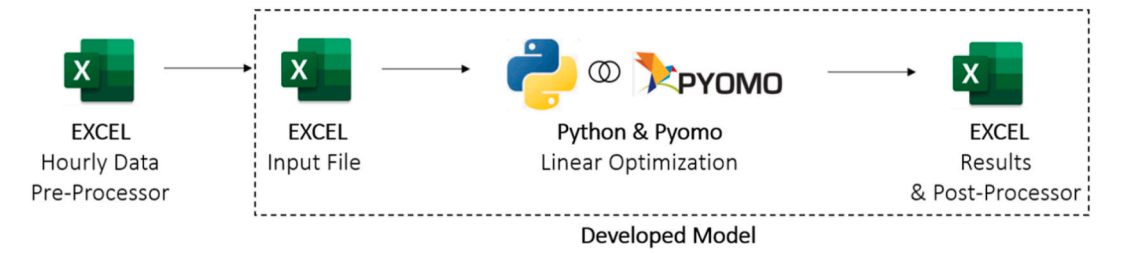


Fig. 3. Illustration of the process flow in the developed optimization model.

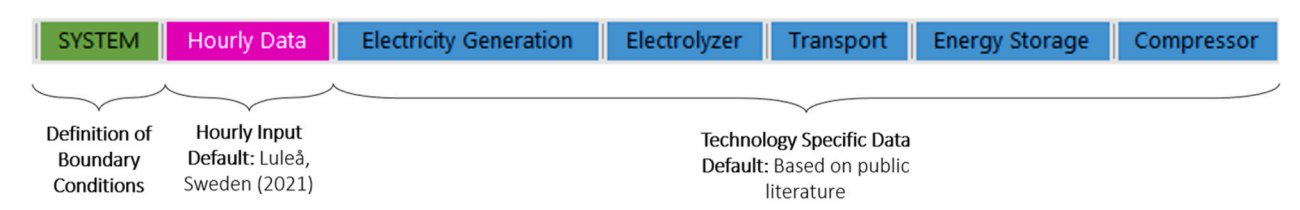


Fig. 4. Input file - overview.

- Economic parameters: Discount rate, Project life span
- Renewable electricity technology (e.g., on/offshore wind power or solar PV): The individual electricity generation sources can be considered or excluded individually. Their maximum installable capacity can be limited.
- Battery System: A battery system can be considered to store electricity from renewable sources. Its maximum installable capacity can be limited.
- Grid connection: A local grid connection can be considered. It either competes freely with the available renewables or a defined share of the annual electricity demand is enforced to be purchased from the grid.
- Hydrogen production technology: An Alkaline or a Proton-Exchange-

Appendix A.

2.2. Optimization model

The optimization model is described as a MILP and solved with the objective to minimize the Net Present Cost (NPC) over the considered project lifespan [29]. The goal of the optimization is to minimize the total system cost over the chosen project lifespan, while accounting for the time value of money by discounting future cash flows. The quantity of hydrogen is predetermined by the input demand. Hence, the objective function aggregates all NPCs throughout the hydrogen supply chain [30]. It is expressed as follows:

$$Minimize \left(NPC_{RE} + NPC_{Grid} + NPC_{Battery} + NPC_{Electolyzer} + NPC_{Conversion} + NPC_{H2\ Storage} + NPC_{Transport} \right) \tag{1}$$

Membrane (PEM) electrolyzer can be chosen as hydrogen production technology.

- Hydrogen gas storage: The user can select one of multiple options to store gaseous hydrogen such as tanks with different pressure levels and geological storages like Depleted Oil Reservoirs or Line Rock
- Hydrogen Transport: The user can let the model optimize for the most feasible type of transport or select a certain type. The considered transport types are via truck (tube trailers) or via pipeline as pressurized gas.

Furthermore, time dependent and location specific data such as wind speeds, solar irradiation, ambient air temperature, electricity spot price, and the hydrogen demand need to be provided to the model. The hydrogen demand can either be based on the actual demand of an existing facility or be estimated, with a key criterion that the data's temporal resolution should match that of the weather and price input data. For this research an hourly time resolution has been chosen. Technology specific cost and performance data for all relevant equipment along the supply chain is required. By default, the parameters for the selectable technologies are pre-defined in the model based on the relevant and publicly available scientific literature in English, Swedish, and German languages. The user can adjust these parameters if needed. An example of the "Electricity Generation"-Sheet can be found in

Where;

NPC_{RE}: NPC of the RE generation capacity [EUR]

 $\mbox{NPC}_{\mbox{Grid}}\mbox{:}\mbox{ NPC}$ for the purchase of electricity from the grid [EUR]

NPC_{Battery}: NPC for the battery storage [EUR]

NPC_{Electrolyzer}: NPC of the electrolyzer (electricity cost are included in

NPC_{RE} and NPC_{Grid}) [EUR]

NPC_{Conversion}: NPC of all compressors [EUR]

NPC_{H2 Storage}: NPC of the hydrogen storage [EUR]

NPC_{Transport}: NPC of hydrogen transmission to the end-consumer

[EUR]

The NPC of the individual stages is calculated under consideration of a discounted value of future cash flows and is expressed as follows:

$$NPC = \sum_{n=0}^{N} \frac{CAPEX_n + REPEX_n + OPEX_n - SALVAGE_n}{(1+d)^n}$$
 (2)

Where;

NPC: Net Present Cost throughout the project economic life span

N: Length of the project period [years]

d: Discount rate

Table 1The Model's optimization variables.

Туре	Variable	Symbol	Unit	Element
Single Value variables (Installed	Onshore Wind	varONW	[kW _e]	$\mathbb{Z}_{\geq 0}$
Capacities)	Offshore Wind Power	varOFW	[kW _e]	$\mathbb{Z}_{\geq 0}$
	Solar PV	varPV	[kW _e]	$\mathbb{Z}_{\geq 0}$
	Battery	В	[kWh _e]	$\mathbb{Z}_{\geq 0}$
	Electrolyzer	E	[kW _e]	$\mathbb{Z}_{\geq 0}^-$
	Compressor	C_x	[kW _e]	$\mathbb{Z}_{\geq 0}$
	Hydrogen Storage	S	[kWh _{LHV}]	$\mathbb{Z}_{\geq 0}$
Hourly Value variables ^a (Energy	Electricity Purchase	grid _h ^{purchase}	[kWh _e /h]	$\mathbb{R}_{\geq 0}$
Flows)	Battery charging	B_h^{charge}	[kWh _e /h]	$\mathbb{R}_{\geq 0}$
	Battery discharging	B_h^{dis}	[kWh _e /h]	$\mathbb{R}_{\geq 0}$
	Hydrogen Production	E_h^{H2}	[kWh _{LHV} / h]	$\mathbb{R}_{\geq 0}$
	Hydrogen Storage charging	S_{h}^{charge}	[kWh _{LHV} / h]	$\mathbb{R}_{\geq 0}$
	Hydrogen Storage discharging	$S_{ m h}^{ m dis}$	[kWh _{LHV} / h]	$\mathbb{R}_{\geq 0}$
Binary variables	Truck utilization	z ^{Truck}	[-]	Binary
(Transport)	Pipeline utilization	$\mathbf{z}^{\text{Pipeline}}$	[-]	Binary

^{**}x – Index for the individual compressor application: x = i, ii, iii, iv.

 $CAPEX_n$: Capital Expenses in year n = 0 [EUR]

 $\mbox{REPEX}_n \mbox{:} \mbox{ Replacement cost required in the year of replacement.}$ [EUR]

 $OPEX_n$: Operational Expense of the component per year. [EUR] $SALVAGE_n$: Remaining value of an asset at the end of the project (n = N), considering a linear depreciation over components' life span. [EUR]

N: Length of the project period [years]

The decision variables (Table 1) are subject to the optimization and can be classified into three types:

- Single value variables: indicate the required capacities across the supply chain,
- Hourly variables: represent the energy flows within the system for a year.
- iii. Binary variables: determine the transport type.

The system's operation is guided by a set of constraints and input parameters, detailed below in alignment with the order of energy flow, starting from primary energy sources (1, 2) and the battery storage (3), then progressing through hydrogen production (4), compression (5),

Table 2Onshore wind power - parameter symbols.

Parameter	Symbol	Unit
CAPEX	CAPEXwind	[EUR/kW]
REPEX	REPEXwind	[EUR/kW]
OPEX	OPEXwind	[EUR/kW/yr]
Lifetime	LT^{wind}	[yr]
Performance factor	η^{wind}	[-]
Surface Roughness	z_0^{wind}	[m]
Turbine hub height	hub ^{wind}	[m]
Power Curve	\overrightarrow{P}	[kW _{out} /m/s/kW _{installed}]
Wind Speed	$c_{\rm h}^{ m wind}$	[m/s]

storage (6), and transport (7) as presented in Fig. 2.

1. Renewable Electricity

The set of parameters and constraints introduced in this part are developed to estimate the required installed capacities for both onshore and offshore wind power and solar PV. Firstly, the electric power output per time step is determined per installed capacity of the different renewable resources, which is required in the energy balance constraints.

For wind power assets (both onshore and offshore) the required set of parameters is presented in Table 2, while the respective values used in the case study are presented in Appendix A.

The measured wind speed data c_h^{wind} is converted from the height of the anemometer to the hub height of the turbine utilizing the concept of surface roughness, identified by Wieringa [31]. The wind speed at the hub height is translated to the hourly power output of the turbine by using the turbine specific power curve that is defined by the manufacturer (see Appendix B). Additionally, to account for system losses of transformers and cables between the turbine and the battery/electrolyzer, an overall system performance factor η^{wind} is applied, which can be described as follows:

$$p_h^{wind} = p_h^{turbine} * \eta^{wind}$$
 (3)

Where,

 $p_h^{turbine}$: Turbine's direct power output before system losses per timestep h [kW_{out}/kW_{installed}].

 p_h^{wind} : Available wind power output per installed capacity [kW_{out}/kW_{installed}].

Generally, the generated electrical power of a wind farm cannot be larger than its installed capacity (rated power) [32]. Therefore, $p_h^{wind} \leq 1$.

Solar PV is another possible source for RE in the model. The electricity generated from PV panels depend on the horizontal irradiation on the panel's surface and the air temperature, which impacts the panel's efficiency. The required parameters are stated in Table 3.

The solar irradiation is measured as total amount of light received by a horizontal surface, the Global Horizontal Irradiance (GHI) in $[W/m^2]$ [33]. The power output of a solar panel is dependent on the total irradiance that is received by the panels' horizontal surface. Therefore, the angle between the sun and the tilted PV panel is computed for every time step by utilizing the method described by Holmgren et al. (PVlib) [34]. Furthermore, it needs to be distinguished between direct and diffuse radiation. The latter is less dependent on the panel's orientation as it represents the amount of reflected radiation from particles and subjects. The concept of Erbs et al. [35] is applied in this research for every time step. It describes the correlation between the diffuse fraction of the total

Table 3 Solar photovoltaic – Parameters.

Parameter	Symbol	Unit
CAPEX	$CAPEX^{pv}$	[EUR/kW]
REPEX	$REPEX^{pv}$	[EUR/kW]
OPEX	$OPEX^{pv}$	[EUR/kW/yr]
Lifetime	LT^{pv}	[yr]
Performance factor	η^{pv}	[-]
Tilt Angle	β	[-]
Azimuth Angle	γ	[-]
Timezone	tz	[-]
Latitute	lat	[deg]
Longitude	long	[deg]
Global Horizontal Irradiation per time step	GHI_h	$[W/m^2]$
Air Temperature per time step	T_{h}^{air}	[deg C]

^a h - Index for every hour per annum: $h = \{1, 2, 3, ..., H\}$; H = 8760.

irradiation and the clearness index, which results in the total radiation perpendicular to the panel's surface, the Plane of Array (POA) irradiance.

By identifying the POA irradiance, the electric power output per installed capacity for every time step can be computed. As Crystalline Silicon cells are the most common PV technology today [36], their performance parameters were applied in this model. Huld and Amilo [37] developed a mathematic description of the panels efficiency in relation to the POA irradiance and the ambient temperature. It is described as follows:

research. The required parameters to describe these constraints are presented in Table 4.

No capital expenditures are assumed for the electricity purchase from the grid, resulting in NPC_{Grid} that solely accounts for yearly operational expenses as stated in the equation below.

$$OPEX = \sum_{h=1}^{H} grid_{h}^{purchase} * \lambda_{h}$$
 (9)

Where,

$$p_h^{PV} = \eta^{PV} * G_h' * \left(1 + k_1 \ln(G_h') + k_2 \ln(G_h')^2 + k_3 \ln(T_h') + k_4 T_h' \ln(G_h') + k_5 T_h' \ln(G_h')^2 + k_6 T_h'^2\right)$$

$$\tag{4}$$

$$G_h' = \frac{POA_h}{1000} \frac{W}{m^2} \tag{5}$$

$$T_h' = T_h^{air} - 25K \tag{6}$$

Where.

 p_h^{PV} : Electric power per installed capacity [kW_{out}/kW_{installed}]. $k_1...k_6$: Technology specific coefficients from Huld et al. [38] (see Appendix B)

For all renewable technologies, the normalized Net Present Cost NNPC in [EUR/kW_{installed}] per installed capacity is calculated by utilizing Equation (2). One-time expenses associated with the transmission of RE to the electrolzyer will be accounted for in the CAPEX, while reoccurring cost, such as power tariffs or maintenance are part of the OPEX of the individual technologies. To compute NPC^{RE} , as part of the objective function, the following relationship is applied:

$$NPC^{ONW,OFW,PV} = NNPC^{ONW,OFW,PV} * varONW, varOFW, varPV$$
 (4)

$$NPC^{RE} = NPC^{ONW} + NPC^{OFW} + NPC^{PV}$$
(5)

Where,

ONW: Indicates parameters for onshore wind power *OFW*: Indicates parameters for offshore wind power *PV*: Indicates parameters for Solar PV

2. Electricity Grid

For each hour, electricity can be purchased from the electricity grid at the respective spot price. Spot price refers to the day-ahead market price of electricity at the time of purchase. In the model, the user can decide whether the purchase of electricity from the grid is in competition with the RE sources or enforce a specified fraction of the total annual electricity consumption to be purchased from the grid. The model prohibits the sale of RE to the grid in order to avoid profit maximization through electricity trading, as it is not the objective of this

Table 4Grid – parameter symbols.

Parameter	Symbol	Unit
Electricity supplied from the grid	grid ^{fraction}	[-]
Maximum grid capacity	G^{max}	[kW]
Hourly electricity purchase price	$\lambda_{\mathbf{h}}$	[EUR/kWh]

 $grid_{h}^{\textit{purchase}}$: Hourly purchased electric energy [kWh/h] λ_h : Hourly electricity spot price [EUR/kWh]

The hourly electric energy purchase is limited by the physical grid connection transmission capacity.

$$\operatorname{grid}_{h}^{\operatorname{purchase}} \ge 0$$
 (10)

$$grid_{h}^{purchase} \le G^{max}$$
 (11)

The model can be enforced to supply a specified fraction of the system's annual electricity demand from the grid. This is expressed in the following constraint. If this constraint is considered, the model determines the most feasible time to purchase electricity from the grid.

$$\sum_{h=1}^{H} \operatorname{grid}_{h}^{purchase} = \operatorname{grid}^{\operatorname{fraction}} * \sum_{h=1}^{H} \left(E_{h}^{electricity} + P_{h}^{C,el} \right)$$
 (12)

Where,

 $E_h^{electricity}$: Electric power demand of the electrolyzer for every time step [kW]

 $P_h^{C,el}$: Electric power demand of all compressors for every time step [kW]

3. Battery Storage

A battery storage can be charged with electricity from the renewable sources to decrease peak power and smoothen the volatile generation. The battery cannot be charged from the grid to avoid electricity arbitrage, which is outside the scope of this research. The required parameters are stated in Table 5.

The normalized Net Present Cost $NNPC^B$ in $[EUR/kW_{installed}]$ per installed capacity is calculated by utilizing Equation (2). To compute the battery's NPC^B the normalized cost is scaled by the installed power capacity of the battery B, which is part of the single value variables. This

Table 5Battery storage – parameter symbols.

Parameter	Symbol	Unit
CAPEX	CAPEX ^B	[EUR/kW]
REPEX	REPEX ^B	[EUR/kW]
OPEX	OPEX ^B	[EUR/kW/yr]
Lifetime	LT^B	[yr]
Cycle Efficiency	η^B	[-]
C-Rating	CR	[-]
Minimum SOC during operation	$SOC^{B,min}$	[-]
Maximum SOC during operation	SOC ^{B,max}	[-]
Initial SOC	SOC_0^B	[-]

relation is expressed as follows:

$$NPC^{B} = NNPC^{B} * B (13)$$

Electricity from the renewables can either be directly used in the electrolyzer or stored in the battery for later usage. The electric charging and discharging power are subject to the installed power capacity. The relation between power and energy capacity is described with the C-Rate of the battery and required as input. With this, the state of charge of the battery can be identified, which can be expressed through the following constraints:

$$p_h^{PV} + p_h^{wind,ONW} + p_h^{wind,OFW} > B_h^{charge} + B_h^{bypass}$$
 (14)

$$B_h^{stored} = B_{h-1}^{stored} + B_h^{charge} - \frac{B_h^{dis}}{n^B}$$
(15)

$$B_{h+1}^{stored} - B_h^{stored} \le CR * B \tag{16}$$

$$B_h^{stored} - B_{h+1}^{stored} \le CR * B \tag{17}$$

Where,

 B_h^{bypass} : Electric power directly used in the electrolyzer [kW]

 B_h^{stored} : Stored energy for every time step [kWh]

 B_h^{charge} : Electric charging power in every time step [kW]

 B_h^{dis} : Electric discharging power in every time step [kW]

Theoretically both discharging and charging could occur simultaneously. However, since the cycle efficiency η^B is considered, it is more feasible to bypass the battery instead. The C-Rate CR describes the charging and discharging power in relation to the battery's energy capacity. However, C-Rates higher than the model's time step (quick charging and discharging) cannot be considered.

The model is required to leave the simulated period with at least the same amount of energy as in the beginning. Furthermore, the stored energy needs to stay within the defined boundaries, which is ensured by the following constraints:

$$B_0^{stored} = SOC_0^B * B \tag{18}$$

$$B_H^{stored} \ge B_0^{stored}$$
 (19)

$$SOC^{B,min} \le \frac{B_h^{stored}}{B} \le SOC^{B,max}$$
 (20)

Where,

 B_0^{stored} : Initial amount of energy stored [kWh]

 $B_{\rm s}^{\rm stored}$: Amount of energy stored at the end of the simulated period [kWh]

4. Electrolyzer

In this research, the costs for water are considered to be neglectable [39]. The model allows to select either an PEM or an Alkaline

Table 6 Electrolyzer - parameter symbols.

Parameter	Symbol	Unit
CAPEX	CAPEX ^E	[EUR/kW]
REPEX	$REPEX^E$	[EUR/kW]
OPEX	$OPEX^E$	[EUR/kW/yr]
Stack lifetime	$LT^{E,stack}$	[h]
Degradation Limit	deg^{E}	[-]
Electrolyzer System Efficiency (LHV)	η^{E}	[-}
Output Pressure	$p^{E,out}$	[Pa]

electrolyzer as hydrogen production technology in the Input Excel Sheet, presented previously. The required parameter to describe the constraints for this stage are presented in Table 6.

The design criteria for the required installed electrolyzer capacity is the year in which the electrolyzer is degraded to its minimum acceptable efficiency \deg^E . This ensures the supply of the given hydrogen demand in all years of the project period. When the degradation reaches the allowable limits, the stack is replaced, accounting for additional expenses.

The normalized Net Present Cost $NNPC^E$ in $[EUR/kW_{installed}]$ per installed capacity is calculated by utilizing Equation (2). To yield NPC^E , the normalized cost is scaled by the installed capacity of the electrolyzer E, similar to the previous stages. This relation is expressed as follows:

$$NPC^{E} = NNPC^{E} * E (21)$$

The energy balance over the electrolyzer accounts for electricity from the renewable sources and from the grid as input and hydrogen as output, assuming a constant efficiency. The produced hydrogen in each hour can be stored for future use or directly be transported to the end-consumer.

$$grid_{h}^{purchase} + B_{h}^{bypass} + B_{h}^{dis} = E_{h}^{electricity} + P_{h}^{C,el,all}$$
 (22)

$$E_{b}^{electricity} * (\eta^{E} - deg^{E}) = E_{b}^{H2}$$
 (23)

$$E_h^{H2} = S_h^{charge} + S_h^{bypass}$$
 (24)

$$E_{\rm b}^{\rm electricity} \le E$$
 (25)

Where,

 $E_h^{electricity}$: Hourly electric energy utilized in the electrolyzer [kWh/h] $P_h^{C.el.all}$: Hourly electric energy utilized by all compressors [kWh/h]

 $S_{h}^{\text{charge}}\text{:}$ Hydrogen flows [kWh_LHv/h] from the electrolyzer to the storage

 S_h^{bypass} : Hydrogen flows [kWh_{LHV}/h] from the electrolyzer to the transport unit

5. Compressors

Compressors are crucial for increasing the volumetric energy density of hydrogen for both storage and transportation. Within the hydrogen supply chain, four compressor applications are considered: (x=i) between the electrolyzer and storage, (x=ii) between the electrolyzer and transport, (x=ii) between storage and transport, and (x=iv) along the pipeline. Multistage Intercooled Compressors are assumed to be used for all applications within the supply chain [24]. The set of parameters presented in Table 7 are required for this stage of the model.

To determine the NPC^{Conversion}, as part of the objective function, the normalized NPC^{C,x} per installed electric capacity for the different compressor applications x = i, ii, iii, iv is calculated by utilizing Equation (2). NNPC^{C,x} is scaled by the single variable representing the installed capacity for each compressor application C_x .

Table 7
Compressor - parameter symbols.

Parameter	Symbol	Unit
CAPEX	CAPEXC	[EUR/kWh]
REPEX	REPEX ^C	[EUR/kWh]
OPEX	$OPEX^C$	[EUR/kWh/yr]
Lifetime	LT^{C}	[yr]
Isentropic Efficiency	η^{is}	[-]
Electric Engine Efficiency	η^{mech}	[-]
Mass losses	loss ^{C,mass}	[-]
Distance between booster compressors	$d^{booster}$	[km]

$$NPC^{C,x} = NNPC^{C,x} * C^{x}$$
 (26)

$$NPC^{Conversion} = NPC^{C,i} + NPC^{C,ii} + NPC^{C,iii} + NPC^{C,iii} + NPC^{C,iv}$$
(27)

The hourly electric compressor power for each application is calculated by assuming an adiabatic compression process and the electric engine efficiency. The compressors' capacities are set equal to the maximum hourly power requirement within the year. The equations presented below are applied to all compressor applications, assuming an adiabatic isentropic compression process [24].

$$P_h^{\text{C,el}} = \frac{P_h^{\text{C,is}}}{\eta^{\text{is}} * \eta^{\text{mech}}} \tag{28} \label{eq:28}$$

$$P_{h}^{C,is} = N_{stages} * \left(\frac{k}{k-1}\right) * Z * T_{av} * Q^{C} * R * \left(\left(\frac{p_{out}}{p_{in}}\right)^{\frac{k-1}{N_{stages} * k}} - 1\right)$$
 (29)

$$N_{\text{stages}} = \text{ROUNDUP}\left(\frac{\log\left(\frac{p_{\text{out}}}{p_{\text{in}}}\right)}{\log(y)}\right)$$
(30)

$$C \ge P_h^{C,el} \tag{31}$$

Where,

 $P_{h}^{\text{C,el}} \colon$ The compressor's electric power requirement for every time step [kW]

 $P_h^{C,is}$: Isentropic power requirement for every time step [kW]

η^{is}: Isentropic efficiency

η^{mech}: Engine efficiency

N_{stages}: Number of compressor stages

k: Heat capacity ratio and is set to 1.41 [40]

Z: Gas compressibility factor at operating pressure at the outlet and ambient temperature

T_{av}: Temperature of the gas [K], set to the average air temperature

Q^C: Mass flow rate of gas through the compressor in [kg/s]

R: Universal gas constant and is set to 4124.01 [J/kg/K] [41]

pout: Outlet pressure of the compressor

p_{in}: Inlet pressure of the compressor

y: 2.1 [40].

For application (x=iv) compressors along the pipeline multiple booster compressors might be required. This depends on the length and the diameter of the pipeline. Therefore, the total installed capacity C^{iv} is the sum off all booster compressors, according to the equations below. These constraints are only relevant if a pipeline is chosen as transport type:

$$C^{i\nu} > P_b^{C,el,i\nu} * n^{booster} \tag{32}$$

Table 8 Hydrogen storage - parameter symbols.

Parameter	Symbol	Unit
CAPEX	CAPEXS	[EUR/kWh]
REPEX	REPEXS	[EUR/kWh]
OPEX	OPEX ^S	[EUR/kWh/yr]
Lifetime	LT^S	[yr]
Operating Pressure	p ^S	[Pa]
Loss per day	loss ^S	[kWh _{LVH} /day]
Minimum SOC during operation	$SOC^{S,min}$	[-]
Initial SOC	SOC_0^S	[-]

$$n^{booster} = \text{ROUNDUP}\left(\frac{d^{pipeline}}{d^{booster}}\right) - 1$$
 (33)

Where.

 $n^{booster}$: Number of required booster compressors

dpipeline: Diameter of the pipeline [km] (see section 7. Transport)

 $P_{n}^{C,el,iv}$: Electric power requirement of the single booster compressor in every time step [kW]

6. Hydrogen Storage

Introducing a buffer between hydrogen production and demand can reduce the total system cost due to smaller required electricity generation and electrolyzer capacities. The optimum capacity of the hydrogen storage depends on multiple factors such as the intermittency of renewable electricity generation, the alignment of the mentioned and the hydrogen demand, and the cost for installing electricity generation and electrolyzer capacity.

In the model, one out of multiple hydrogen storage technologies can be considered by adjusting the parameters presented in Table 8. These parameters are predefined for four commonly discussed storage technologies, such as (i) Pressurized Tank Type I, (ii) Pressurized Tank Type III, (iii) Depleted Oil Reservoir, (iv) Lined Rock Cavern.

Generally, the storage of hydrogen in tanks allows to have the storage in close approximation to the final demand. The main difference between the two tank types is the pressure levels. While Type III Tanks are preferred when available space is limited due to their higher pressure level, Type I Tanks are the most common storage for stationary applications [42]. Depleted Oil Reservoirs and Lined Rock Caverns are geological reservoirs utilizing natural underground formation and are usually connected to lower investment costs than tanks [43].

Similar to the stages introduced previously, the NNPC^S per installed capacity in [EUR/kWh] is determined using Equation (2) and thereafter scaled with the single variable S, which represents the installed storage capacity in [kWh]:

$$NPC^{S} = NPC^{S} * S (34)$$

The amount of hydrogen stored in each time step is the result of the balance between charging and discharging the storage, as well as losses due to leakages. Losses are dependent on the amount of stored hydrogen in the respective hour. Based on the most feasible decision, hydrogen can be stored for later or directly forwarded to the transport. The model determines the required storage capacity based on the maximum amount of stored hydrogen within a year.

$$S_h^{\text{stored}} = S_{h-1}^{\text{stored}} + S_h^{\text{charge}} - S_h^{\text{dis}} - S_{h-1}^{\text{stored}} * \frac{\text{loss}^S}{24}$$
 (35)

$$S_h^{\text{stored}} \le S \tag{36}$$

$$S_h^{\text{stored}} \ge S * SOC^{S,\min}$$
 (37)

$$S_0 = SOC_0^S * S \tag{38}$$

Table 9
Truck - parameter symbols.

Parameter	Symbol	Unit
Hourly Truck Costs (Leasing)	TruckLeasinghourly	[EUR/h]
Average Speed	v ^{truck}	[km/h]
Loading and Unloading Requirement	LoadingTime	[h]
Travel Distance	d ^{truck}	[km]
Truck Pressure	p ^{truck}	[Pa]
Truck Capacity	m ^{truck}	[kg/truck]

$$S_{H} \ge S_{0} \tag{39}$$

Where,

S_b^{stored}: Amount of energy [kWh_{LVH}] stored per hour h

SOC₀^S: State of charge of the storage at hour 0

S_H: Energy content in the final hour of the optimization period.

7. Transport

The transport options in the model are limited to hydrogen transport via pipeline or truck, as the scope of the research is domestically produced and utilized gaseous hydrogen. Through the use of binary variables, the model can optimize the economically most feasible transport type. However, the user is able to enforce the use of a certain type, as factors such as construction permits [17], geological suitability [25], required flexibility [27], etc., are not considered here.

The $\mbox{NPC}^{\mbox{\it Transport}}$ is calculated based on Equation (2) with respect to the following constraints:

$$NPC^{Transport} = z^{Truck} * NPC^{Truck} + z^{Pipeline} * NPC^{Pipeline}$$
 (40)

$$1 = z^{Truck} + z^{Pipeline} \tag{41}$$

For transporting hydrogen via tube trailers, the following parameters stated in Table 9 are required.

In this research, it is assumed that trucks are leased, and therefore only operational expenses are considered for the NPC calculation:

$$OPEX = \frac{TruckLeasing}{m^{truck} * LHV} \left(\frac{d^{truck}}{v^{truck}} + LoadingTime \right) * \sum_{h=1}^{H} Demand_{h}$$
 (42)

Where.

Demand_h: Hourly hydrogen demand [kWh_{LHV}/h]

For calculating the economic and physical relations of a pipeline as transport option, the parameters presented in Table 10 are required.

Installing a pipeline for hydrogen transport incurs initial investment and operational expenses.

The pipeline's diameter directly affects the costs and the useable flexible linepack as an additional hydrogen storage option. Baufemé et al. [44] found that the cost for hydrogen pipelines can be described by a quadratic equation as follows:

$$ext{CAPEX}^{Pipeline} = \left(1500000*D^{Pipeline^2} + 860500*D^{Pipeline} + 247500
ight) \ * d^{Pipeline}$$

(43)

$$OPEX^{Pipeline} = opex^{Pipeline} * CAPEX^{Pipeline}$$
 (44)

Where,

D: Pipeline Diameter [m]

Table 10 Pipeline - parameter symbols.

Parameter	Symbol	Unit
OPEX as fraction of CAPEX	opexPipeline	[-]
Lifetime	$LT^{Pipeline}$	[yr]
Required Output Pressure	p ^{out}	[Pa]
Operational Pressure	p^{op}	[Pa]
Flow Velocity	$v^{Pipeline}$	[m/s]
Initial SOC of the Linepack	$SOC_0^{Pipeline}$	[-]
Pipeline Distance	d ^{Pipeline}	[km]
Maximum Distance between Booster Stations	$\mathbf{d}^{\mathrm{booster}}$	[km]

The pipeline's diameter can either be given by the user of the model as input parameter or it can be determined using the simplified flow model described below [44]. The design criteria is the maximum amount of hydrogen that is transported in one timestep throughout a year.

$$p_{av}^{pipeline} = \frac{2}{3} \left(\frac{p^{op^3} - p^{out^3}}{p^{op^2} - p^{out^2}} \right)$$
 (45)

$$Q_{max} = \frac{\max(D_h)}{\text{LHV}_{H2} * \rho_{av} * 3600}$$
 (46)

$$D^{\textit{Pipeline}} = \sqrt{\frac{4 * Q_{\textit{max}}}{V^{\textit{Pipeline}} * \pi}} \tag{47}$$

Where:

 $p_{av}^{\text{pipeline}}\text{:}$ Average pressure over the pipeline [Pa] at average ambient temperature

 Q_{max} : Maximum volume flow within a year [m³/s] ρ_{av} : Density of the gas at average pressure

The simplied flow model does not account for pressure drops due to friction within the fluid and between the fluid and the pipe wall [44]. Therefore, the obtained diameter needs to be validated by calculating the pressure drop of the flow between the inlet and the next booster station or between inlet and outlet if the pipeline distance is short enough so that no booster stations are required.

The general flow equation for steady state gas flow, assuming a horizontal pipe, is utilized [45]:

$$p^{out,calc} = \sqrt{p^{op^2} - \left(\frac{Q_{max} * p_{atm}}{\sqrt{\pi^2 * \rho_{air} * 64^{-1}} * T_n}\right)^2 * \frac{f * S * d^{pipeline} * T_{av} * Z}{\left(D^{pipeline}\right)^5}}$$
(48)

$$f = \frac{0.3164}{RE^{0.25}} \tag{49}$$

$$RE = \frac{4 * Q_{max}}{\pi * D^{pipeline} * V_{kin}}$$
(50)

Where:

p^{out,calc}: Calculated outlet pressure at the outlet [Pa]

 p_{atm} : Atmospheric pressure = 101 325 Pa

 T_n : Standard Temperature (273.15K)

 ρ_{air} : Air density at p_{atm} and T_n [kg/m³]

S: Gas specific gravity for hydrogen = 0.0696

Z: Gas compressibility factor at $p_{av}^{pipeline}$.

f: Friction factor for turbulend flow [46]

RE: Reynoldsnumber for a circular pipe [45]

 v_{kin} : Kinematic velocity of hydrogen at Standard Temperature and Pressure (STP) = $9.84 \times 10^{-5} \, [\text{m}^2/\text{s}]$ [45]

The calculated outlet pressure $p^{out,calc}$ need to be equal to or larger than the minimum required outlet pressure at the demand. If this condition is not met, the diameter is increased iteratively and the previous steps are repeated:

if:
$$p^{out,calc} < p^{out}$$
 then: $D^{Pipeline} = D^{Pipeline} + 0.01 [m]$ (51)

The pipeline's average pressure can vary between its minimum and maximum operational pressure, allowing storage of useable quantities of hydrogen as flexible linepack. Therefore, the pipeline can be seen as a supplement to hydrogen storage, providing a means of storing and transporting hydrogen in a flexible manner. The flexible linepack is

determined according to the following set of equations:

$$\Delta p^{\text{Linepack}} = p_{\text{max}}^{\text{pipeline}} - p_{\text{min}}^{\text{pipeline}}$$
 (52)

$$V^{\text{H2,flexible}} = d^{\textit{Pipeline}} * \frac{\pi * D^{\text{Pipeline}^2}}{4} * \frac{1}{p_n} * \frac{T_n}{T_{av}} * \left(\frac{p_{max}^{\text{pipeline}}}{z_{max}} - \frac{p_{min}^{\text{pipeline}}}{z_{min}} \right)$$
 (53)

$$P^{\text{Linepack}} = V^{\text{H2,flexible}} * \rho_n * LHV_{\text{H2}}$$
 (54)

$$P_{h}^{\text{stored}} = P_{h-1}^{\text{stored}} + S_{h}^{\text{dis}} + S_{h}^{\text{bypass}} - D_{h}$$

$$(55)$$

$$P_{\rm b}^{\rm stored} < P^{\rm Linepack} * z^{\rm Pipeline}$$
 (56)

$$P_{H}^{\text{stored}} \ge P_{0}^{\text{stored}} \tag{57}$$

Where,

p_n: Average pressure [Pa]

T_n: Average temperature [K]

 ho_n : Average density [kg/m3] of the hydrogen in the pipeline at STP z_{max} and z_{min} : Compressibility factors of hydrogen at maximum and minimum mean pressure at average ambient temperature, respectively

 $P_h^{\rm stored} :$ Amount of hydrogen stored as flexible line pack for each hour h

 P_0^{stored} : Energy content at hour 0

 P_H^{stored} : Energy contents in the final hour of the optimization

A more comprehensive mathematical description of the presented constraints and the parameter values can be found in Appendices A and B. In the Results and Post-Processor EXCEL File, cashflow analyses are performed for all stages of the supply chain which results in the levelized costs of electricity generation, hydrogen production, compression, storage, and transport. Screenshots with examples of the visualized results can be found in Appendix C.

3. Case study: Swedish Iron and Steel industry

To demonstrate the application of the developed methodology, a case study in the Iron and Steel industry in northern Sweden, in the surrounding of Luleå, is investigated. Therefore, data for a representative company, hereafter referred to as "The Company", is collected and fed into the model. The purpose of the study is to investigate the layout, cost, and dispatch of the required hydrogen supply chain in multiple scenarios, if parts of The Company's fossil fuel demand is to be supplied

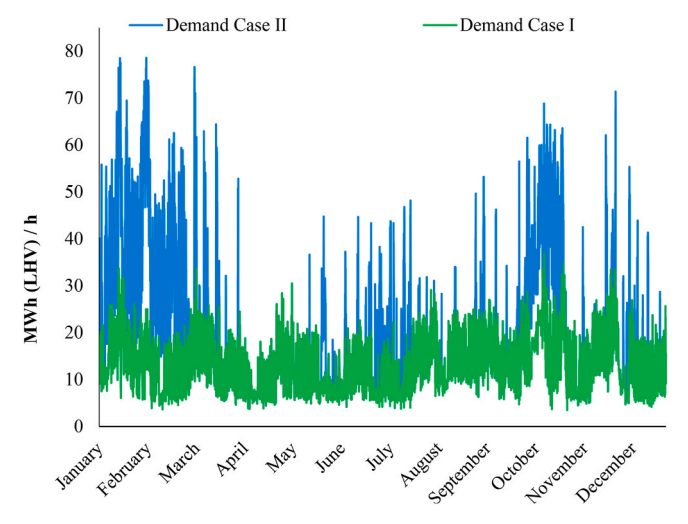


Fig. 5. Energy demand for both Demand Cases throughout the year.

with domestically produced, low carbon hydrogen. At present, The Company requires heat from furnaces and steam from boilers for its processes, which are powered by light furnace oil and liquified petroleum gas. Further details about the case study cannot be provided due to confidentiality reasons related to The Company's operations.

3.1. Data

Two different demand cases are investigated to study the impact of the fluctuation of the demand on the design of the hydrogen supply chain. The hourly energy consumption data for those cases is presented in Fig. 5 and Table 11. When substituting fossil fuel consumption, it is assumed that the same amount of energy (Lower Heating Value LHV) will be required in each time step:

- Demand Case 1: In this case it is assumed that all fossil fired furnaces for heat generation can be switched to hydrogen. However, the steam boilers, used for steam generation in times when excess heat from the remaining processes is insufficient are assumed to be electrified instead. Hence, their energy consumption is excluded from the hydrogen demand and not discussed further (see Fig. 6).
- Demand Case 2: In this demand case, it is assumed that both furnaces and steam boilers are switched to hydrogen (see Fig. 7).

In Sweden, the electricity pricing system is split into four geographic pricing-zones. The hourly electricity spot prices are defined per price area. The Company is located in the electricity pricing area SE1. For the year under consideration, the average electricity spot prices in SE1 are 30 EUR/MWh. Notably, these prices exhibit a distinct daily pattern with peak prices in the morning and afternoon, and lower prices at night as shown in Fig. 8 [47].

The average wind speed at Northern Sweden in 2021, both onshore and offshore, was 3.5 m/s and 5.9 m/s, respectively [48,49]. Offshore wind speeds, being less variable than onshore speeds, experience fewer short-term and seasonal fluctuations, with the highest wind speeds occurring in spring and autumn. For onshore, the wind speed was assessed for the year 2021 from the weather station: "Luleå-Kallax Flygplats" with the station ID 162860 [48] with hourly resolution. In case of offshore, the measured wind speed data is considered from the weather station: "Rödkallen A" with the station ID 162790 [49]. The seasonal average wind speeds for every hour of the day are displayed in Fig. 9 (A) and (B). It represents an average day with its wind speed variation per season. Fig. 9 (C) presents the average wind speeds for both the onshore and the offshore sites.

Solar irradiation reaches its zenith, averaging 500 W/m² at noon, while it diminishes to negligible levels in winter months. Hourly measurements for 2021 are provided by SMHI and are measured in the weather station "Luleå Sol" with the station ID 162015 [50]. The daily average variation of GHI for the different seasons is presented in Fig. 10 (A) and the monthly average GHI (B) is displayed.

The area around the Company were screened for geological formations that can be suitable to store gaseous hydrogen. Depleted oil or gas reservoirs are scarce in Sweden and no useable reservoirs are available in the northern part of Sweden [51]. Consequently, the option of storing hydrogen in a Depleted Oil Reservoir is excluded in this analysis. However, multiple rock caverns were found in the area. The selected cavern is a depleted mine, which is to be upgraded for the storage of pressurized gas. The investment costs for the Lined Rock Cavern are presented in Appendix A. The transport distance between the chosen geological hydrogen storage and the final consumption is 30 km by pipeline or 50 km by truck due to the available road network.

The industrial site and the land in close approximation to the case company provides sufficient available space to install an electrolyzer and large-scale hydrogen tank storage tanks and thus, the transport distance can be kept to a minimum. It is assumed that in this case, the distance will always be covered by a pipeline with a length of 500 m,

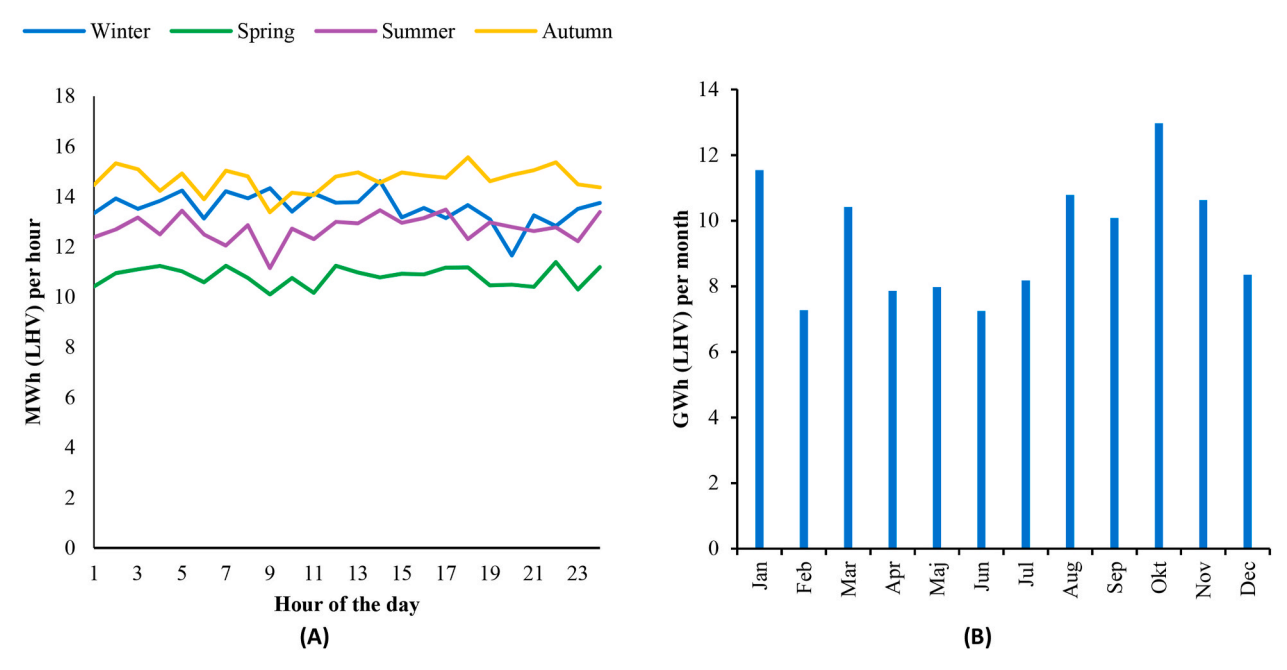


Fig. 6. Hydrogen demand I - Daily average over a season (A) and total monthly (B).

Table 11
Key data for Demand Cases 1 and 2.

	Annual Demand [GWh _{LHV}]	Average Demand [MWh _{LHV} /h]	Peak Demand [MWh _{LHV} /h]
Demand Case 1	113	13	37
Demand Case 2	171	20	79

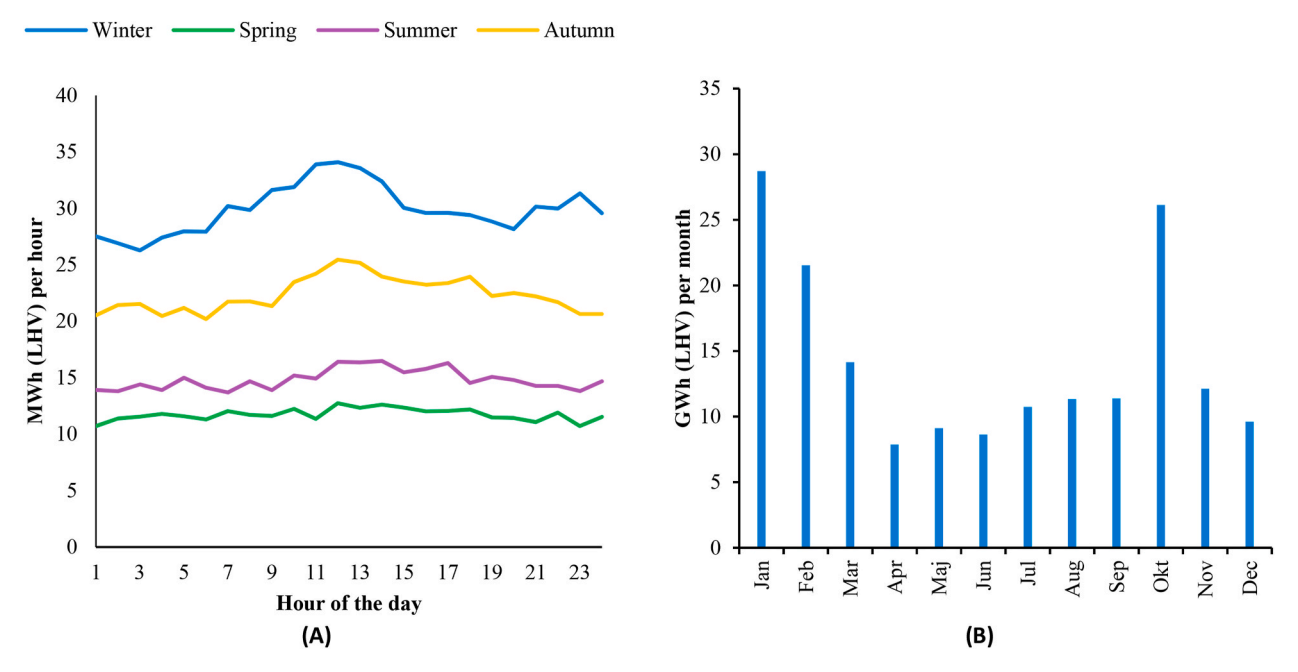


Fig. 7. Hydrogen demand II - Daily average over a season (A) and total monthly (B).

which prevents utilizing a flexible linepack due to the short distance. In the case study, a PEM electrolyzer is chosen to be used in all scenarios, as this technology is considered the most suitable in combination with fluctuating RE [52]. Therefore, the electrolyzer can operate in its full capacity range [53].

3.2. Scenarios

Considering the variety of diverse demand patterns, electricity sources, hydrogen storage technologies, and transport types, multiple scenarios are developed and tested in the model. As part of the research, 25 different scenarios were identified and analysed. Each scenario represents a unique set of boundary conditions. Due to space limitations, six

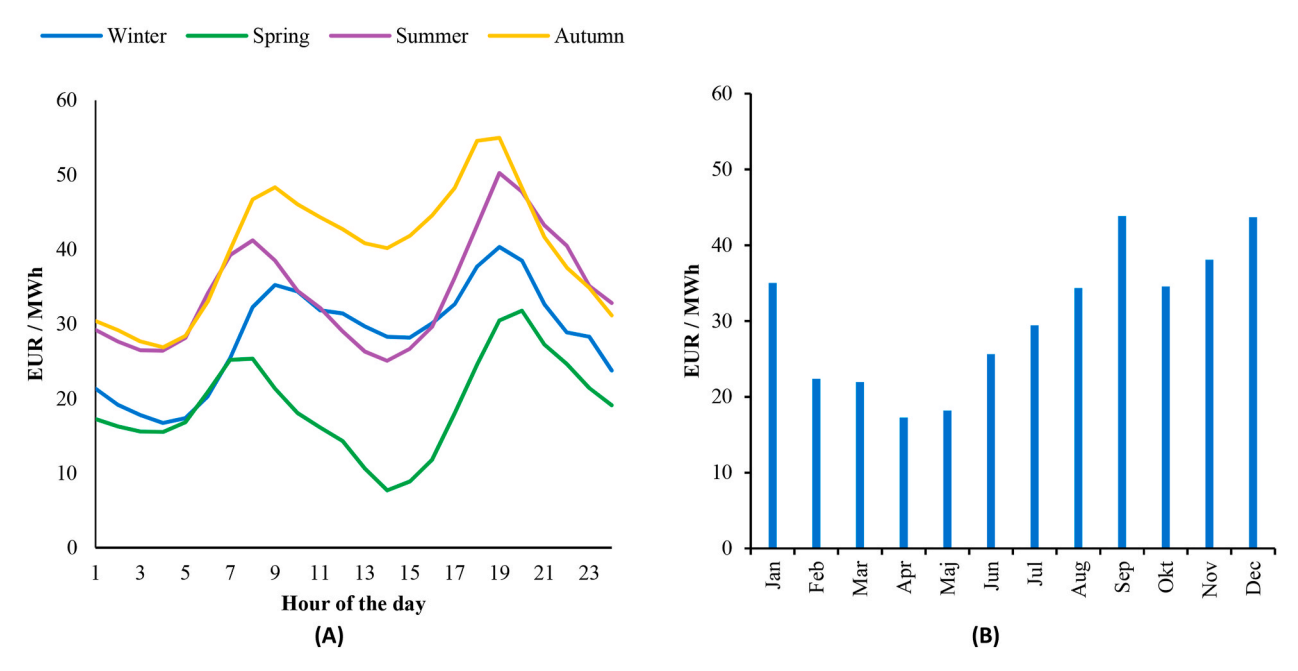


Fig. 8. Electricity Spot Price - Daily Average over each season (A) and Monthly Average (B).

out of those scenarios are presented in further detail in this research paper. Both demand cases are seen as equally probable. Therefore, all chosen boundaries regarding electricity sources, hydrogen storage technologies, and transport types are computed in both demand cases to allow a direct comparison, while the underlying cost and performance parameters for each technology are unchanged. This implies that the cost for electricity transmission per installed unit is assumed to be the same for all chosen boundaries. Furthermore, the impact of the type of electricity generation and the hydrogen storage type are considered of high importance for the audience. From all tested scenarios, it can be seen that the transport type has only a minor impact on the layout and dispatch of the supply chain and is therefore not highlighted specifically.

A summary of all presented scenarios can be found in Table 12.

Scenario 1: This scenario introduces different electricity sources in free competition. It incorporates a combination of various electricity sources while storing hydrogen in a Lined Rock Cavern and transporting it via pipeline to the end-consumer. The focus is on satisfying Demand Case 1.

Scenario 2: Building upon Scenario 1, this scenario maintains the same boundary conditions but shifts the emphasis to Demand Case 2. **Scenario 3**: This scenario mandates that no electricity is purchased from the grid; instead, all electricity must be supplied from newly installed RE sources.

Scenario 4: Similar to Scenario 3, this scenario considers the installation of RE sources, but the emphasis is on satisfying Demand Case 2.

Scenario 5: This scenario, while relying on an electricity supply solely from RE sources, adopts a different approach to hydrogen storage. Hydrogen is stored in tanks located in close proximity to the demand and is subsequently transported to the factory via a 500-mlong pipeline.

Scenario 6: Has the same boundary conditions as Scenario 5 but instead, Demand Case 2 needs to be satisfied.

4. Results

The resulting economics, layout, and dispatch for the selected scenarios are presented in this section. The section starts with the presentation of the optimum layout, followed by the dispatch, the economic

analysis, and ends with the sensitivity analysis.

4.1. Optimal layout

The alteration of constraints in the electricity supply system and storage types significantly influences the optimal configuration of the hydrogen supply chain. The outcomes of the scenarios are presented in Table 13. It is worth noting that only in two out of the 25 calculated scenarios and in none of the presented ones, a battery storage system was chosen to be installed in the optimal layout. Similarly, only one out of the 25 scenarios resulted in solar PV capacity to be installed, while none of the presented ones includes this renewable technology as part of their resulted layout.

Figs. 11–13 showcase the installed capacities of the key components throughout the supply chain. The results for the scenarios are presented in groups depending on the considered Demand Case to allow for a better comparison. Therefore, Sc1, Sc3, and Sc5 are presented together as Demand Case I is considered, while Demand Case II is represented in Sc2, Sc4, and Sc6.

In Sc1, the free competitive environment among electricity sources leads to hydrogen supply that relies entirely on electricity obtained from the grid. A hydrogen storage system with a capacity of 1540 MWh is used for peak shaving and balancing intermittent hydrogen demand. This is approximately a quarter of the required storage capacity for the other scenarios that supply Demand Case I. Also, the electrolyzer, with an electric capacity of 41 MW, is approximately half as large as in Sc3 and Sc5.

In Sc2, 58% of the system's electricity requirement is supplied from the grid, while the remainder is generated from 109 MW of additional wind power capacity, of which 84% are onshore and the rest offshore. The electrolyzer and storage capacity are significantly higher compared to Sc1. Still, the utilization of the grid leads to the smallest electrolyzer capacity among all scenarios that consider Demand Case II.

In Sc3 the usage of electric power from the grid is restricted, leading to the optimal configuration being based on wind power. The capacity is split 60% and 40% between onshore and offshore wind power, respectively. The utilization of intermittent RE sources in this scenario demands 82% more electrolyzer capacity, double the compressor capacity, and nearly quadrupled capacity of the geological storage compared to Sc1 (in which electricity was exclusively purchased from the grid). The

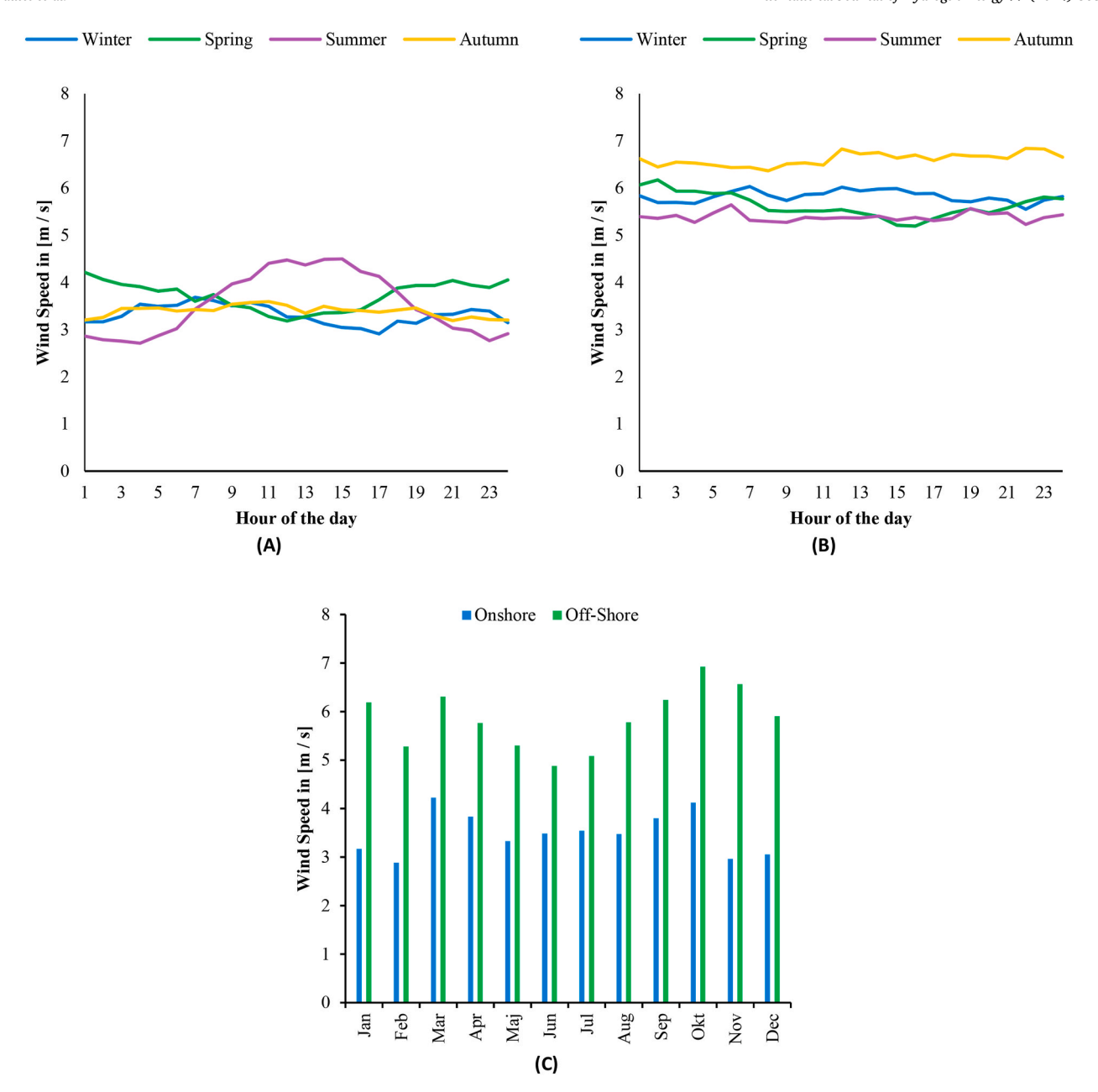


Fig. 9. Wind Speed - Daily Average over a Season for Onshore (A), Offshore (B), and Monthly Average for both (C).

upstream supply chain layout does not affect the diameter of the pipeline, and the incorporation of flexible linepack provides an additional storage capacity of 10 MWh_{LHV}, which, however, is marginal compared to the geological storage with a capacity of 6 GWh_{LHV}.

Sc4, with approximately two thirds of the total wind power capacity built onshore, requires an electrolyzer with 48% of the total RE capacity and is significantly larger than in Sc2. The storage capacity almost doubles compared to Sc2. Sc1 represents the scenario with the largest hydrogen storage requirements among all the calculated cases.

In Sc5, in which hydrogen can only be stored in tanks, the installed capacities for onshore and offshore wind power are 3% and 1% smaller than in Sc3, respectively. However, the capacity of the electrolyzer has increased by 9% and the compressors by over 100% while the storage capacity decreases by 5%.

In Sc6, electricity is exclusively supplied by onshore wind power with almost triple the installed capacity of Sc4. Large electrolyzer and compressor capacities are required. However, with 9 GWh_{LHV} , the installed storage capacity is significantly lower than in Sc2 and Sc4.

Therefore, this scenario requires by far the largest electric power and electrolyzer capacity while minimizing the need for storage.

Generally, it can be seen that Scenarios 1, 3, and 5, considering Demand Case I require significantly lower capacities than Scenarios 2, 4, and 6, which supply Demand Case II.

4.2. Optimal dispatch

The optimal dispatch of a supply chain is closely linked to its layout. Due to the difference in hydrogen demand between the two Demand Cases, the scenarios are clustered according to the respective Demand case to allow for a meaningful comparison. Fig. 14 visualizes the yearly electricity generation and purchase per scenario. It is worth noting that electric energy is partially curtailed. The amount of curtailed energy is the difference between generated and utilized energy and can be seen in Fig. 15.

In Sc1, the electricity supply is solely supplied from the grid. During periods of higher prices, particularly in the morning and evening, less

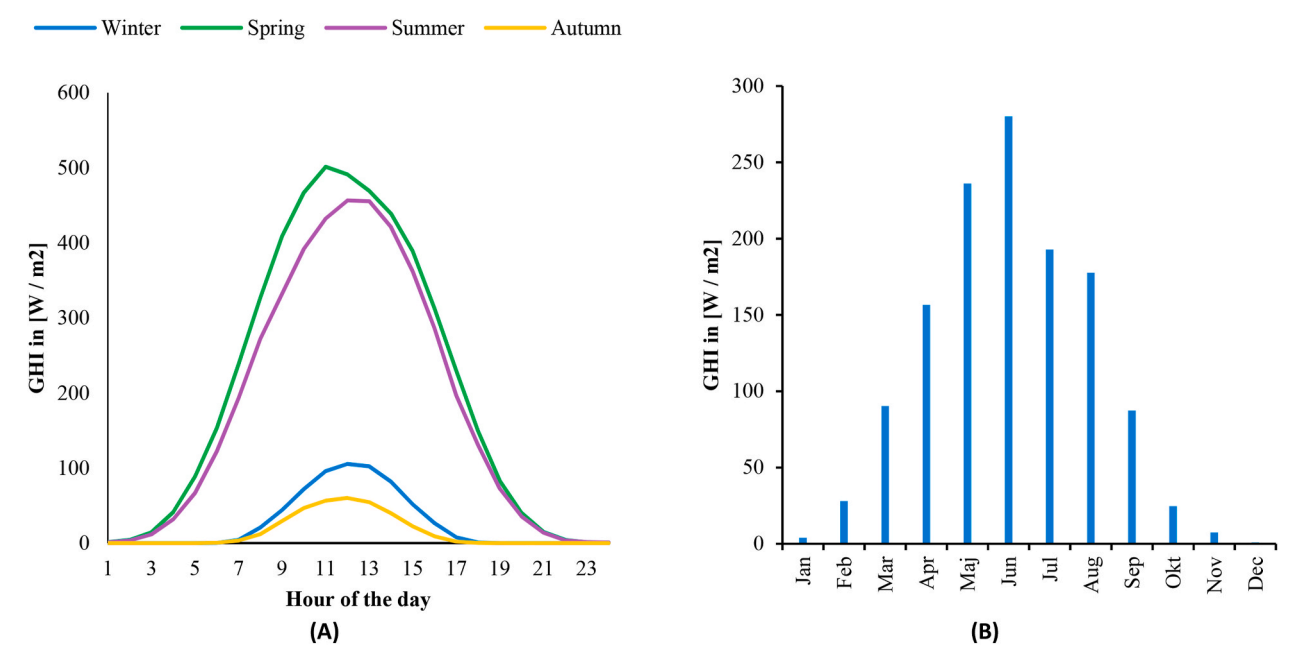


Fig. 10. Global horizontal irradiance - Daily average over a season (A) and monthly average (B).

Table 12Summary of the presented scenarios.

Scenario	Hydrogen Demand Case	Electricity Supply	Storage	Transport
Sc1	Case 1	Free	Geological	Pipeline (30 km)
Sc2	Case 2	Free	Geological	Pipeline (30 km)
Sc3	Case 1	RE only	Geological	Pipeline (30 km)
Sc4	Case 2	RE only	Geological	Pipeline (30 km)
Sc5	Case 1	RE only	Tank	Pipeline (0,5 km)
Sc6	Case 2	RE only	Tank	Pipeline (0,5 km)

electricity is purchased, resulting in a reduced hydrogen output from the electrolyzer and increased utilization of the storage system. Consequently, the electrolyzer's capacity factor reaches 80% in this scenario.

In Sc2, the limited grid connection demands additional electricity to be generated from wind power. During autumn and winter, the hydrogen demand is high, requiring an almost constant purchase of electricity from the grid. In contrast, during the spring, when demand decreases but wind speeds are high, electricity is mainly purchased during times of low prices, to produce hydrogen at low cost and store it. In contrast to Sc1, the capacity factor of the electrolyzer is decreased to 68%, while only 1% of the annually generated RE is curtailed.

In Sc3, electricity generation relies solely on fluctuating wind speeds, which exhibit short-term and seasonal variation. The onshore and offshore wind farms operate at capacity factors of 23% and 33%, respectively, and 18% of the yearly electric energy is curtailed due to the oversized renewable generation capacity in comparison to the electric capacity of the electrolyzer. The electrolyzer in Sc3 has a calculated capacity factor of 47%.

In Sc4, the amount of curtailed energy decreases by 15% since time periods of high wind speeds generally align with an increased hydrogen demand (when considering Demand Case I) and additional storage capacity is comparably feasible. This leads to a similar capacity factor for the electrolyzer as in Sc3.

In Sc5, like in Sc3, the short term and seasonal variation of electricity generation negatively affect hydrogen production. Furthermore, the storage of hydrogen in tanks is comparably cost intensive. To allow for a reduced storage capacity, the electrolyzer capacity increases compared to Sc3. However, this also leads to a reduction of the electrolyzer's capacity factor to 42%.

In Sc6, the electrolyzer's capacity factor decreases drastically to 20%, while 64% of the annual generated electric energy is curtailed. This, however, is economically more feasible than increasing the storage capacity as the storage of hydrogen in tanks is comparably cost intensive. In this scenario, the cost for storing hydrogen have a significantly higher impact on the layout and dispatch of the supply chain than in Sc5, as the hydrogen demand in Demand Case is more volatile with higher

Table 13Optimal installed capacities for each scenario.

Scenario	Onshore Wind	Offshore Wind	Grid Utilization	Electrolyzer	Compressor	Hydrogen Storage	Pipeline Diameter
	[MW]	[MW]	[% of total Energy]	[MW]	[MW]	[MWh _{LHV}]	[m]
Sc1	_	_	100	41	0.2	1540	0.08
Sc2	92	17	58	92	0.7	24 280	0.12
Sc3	95	62	_	75	0.5	5940	0.08
Sc4	213	108	_	152	1.2	42 120	0.12
Sc5	92	62	_	81	1.1	5660	_
Sc6	621	_	_	253	3.3	8930	_

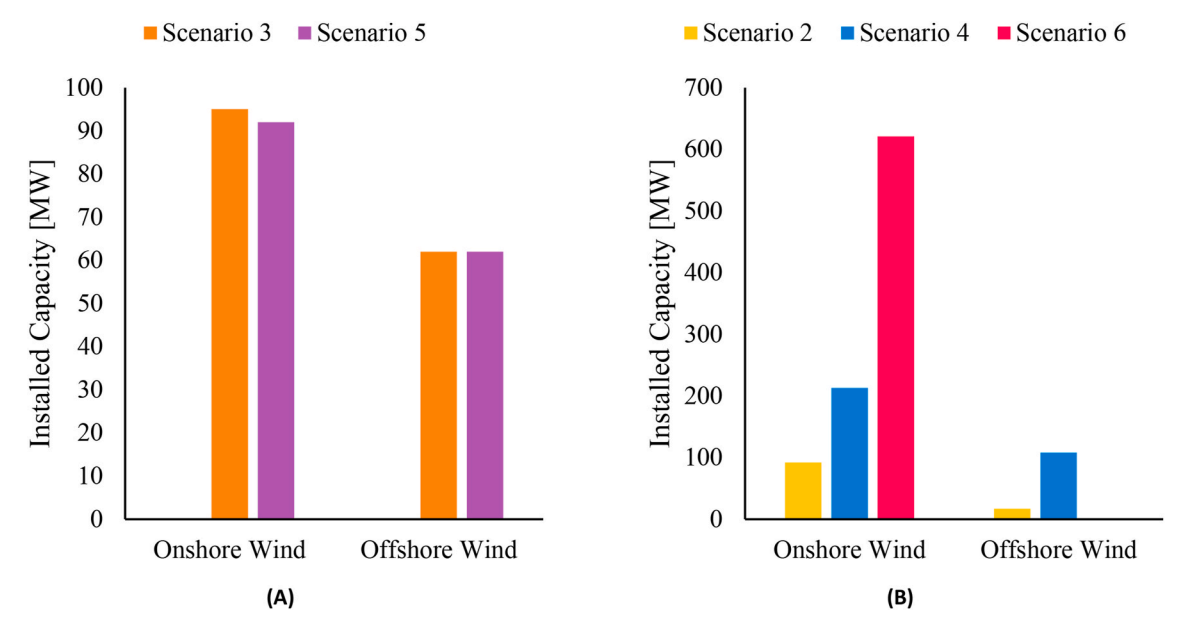


Fig. 11. Installed Renewable Generation Capacity for Scenarios considering Demand case I (A) and Demand Case II (B).

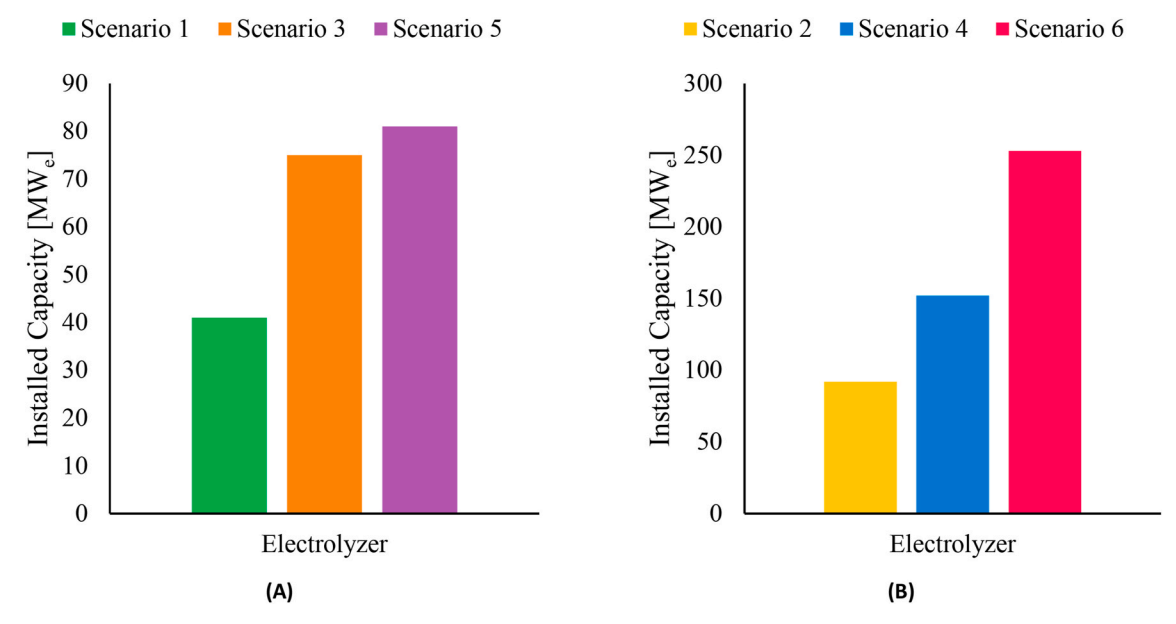


Fig. 12. Installed Electrolyzer Capacity for Scenarios considering Demand case I (A) and Demand Case II (B).

peak consumption. Consequently, more energy needed to be stored over a longer period of time or the hydrogen production capacity has to be increased drastically.

Fig. 15 illustrates the monthly energy utilization and the RE generation of the system for both Demand Cases. Here, the energy utilization in Sc1 is equal to the purchase of electricity from the grid, while for all other scenarios, the difference between the sum of generated and purchased electricity, and electricity that is utilized is considered as curtailed.

The hydrogen demand varies throughout the year for both Demand cases. While in all scenarios with Demand case 1, the hydrogen production aligns with the seasonal demand variation (see Appendix C), the hydrogen production in Sc2 and Sc4 is smoothened throughout the year, due to the application of the geological storage to shift demand and supply over seasons, while it is more volatile in Sc6 to the decreased storage capacity. The total amount of produced hydrogen exceeds the total demand in all scenarios. This is attributed to hydrogen storage

losses and the larger amount of hydrogen stored seasonally, especially in Sc2 and Sc4 as it can be seen in Fig. 16.

In Scenario 1, the hydrogen storage is utilized hourly to monthly, balancing the intermittency of hydrogen demand and price fluctuations. The storage capacity in Scenario 3 and Scenario 5 are significantly larger than that of Scenario 1. In these scenarios the storage is utilized to manage short-term and seasonal fluctuations in both electricity generation and hydrogen demand.

Demand Case 2 has high demand peaks in the beginning of the year and in October. The rest of the year, the hydrogen demand is similar to Demand Case 1. This results in a seasonal use of the storage, in which the storage gets continuously charged during times of low demand to supply periods with demand peaks. In contrast to Sc2 and Sc4, the storage capacity in Sc6 is comparably small and cycled more often throughout the year. It is worth noting that the demand peaks in Demand Case 2 occur mostly in January, requiring the storage to be filled at least by 80% in the first time step of the optimization.

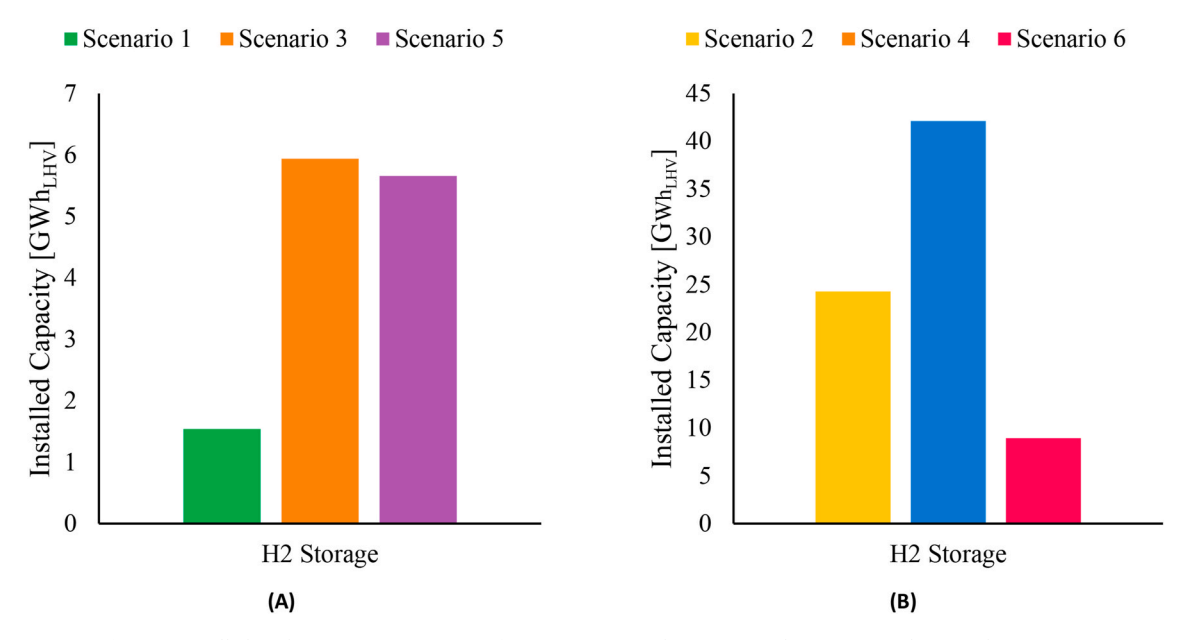


Fig. 13. Installed Hydrogen Storage Capacity for Scenarios considering Demand case I (A) and Demand Case II (B).

4.3. Economic analysis

The chosen boundary conditions and Demand Cases are leading to a substantially different LCOH. Comparing Sc1, Sc3, and Sc5 with Sc2, Sc4, and Sc6 shows that the LCOH for Demand Case 1 is approximately half of Demand case 2. In all scenarios, the generation and procurement of electricity, coupled with the electrolyzer, are the primary cost drivers of the supply chain, as presented in Table 14 and Fig. 17.

The presented LCOH does not account for any revenue stream that could be generated by selling additional hydrogen when demand is low, selling RE on the spot market, or selling side products such as heat and oxygen. However, this can be seen as an additional option to lower the total system costs in further research.

The installation of the electrolyzer is the major cost driver in most of the scenarios. In Sc3 and Sc4, in which electricity is solely generated from the renewable sources, the electrolyzer accounts for more than half of the total system cost. This is due to the increased electrolyzer capacity when powered by fluctuating renewable generation. When comparing Sc5 and Sc6 with the other scenarios, the hydrogen storage in tanks has a significantly higher cost impact on the system cost than the utilization of geological formations. Furthermore, the cost impact of the storage, regardless of its type increases when considering Demand Case II in comparison to Demand Case I, as more hydrogen needs to be stored over a longer period to meet the seasonal demand peaks.

4.4. Sensitivity analysis

From the previous section it can be seen that the results vary significantly when adjusting the boundary conditions described in the scenarios. To understand the impact of uncertainties connected to these boundary conditions and the chosen parameter, a sensitivity analysis is conducted. The impacts of the following three key parameters on the final LCOH are tested: (i) the electrolyzer efficiency, due to the wide variety of values found in the relevant literature; (ii) the replacement cost for the electrolyzer stack during the project lifetime due the uncertainty of the technology's forecasted prices; (iii) the capital investment cost for the geological storage, since the technology is currently not widely used for storing hydrogen in large scale.

All sensitivity variables vary between -10 % and +10 % of the originally utilized value and are fed into the optimization as input variable, while keeping the remaining parameters constant and equal to

Scenario 1. As new simulations are performed with every sensitivity variable, their variation not only impacts the economics but also the layout and dispatch of the optimum supply chain. The results of the sensitivity analysis are presented in Fig. 18.

The efficiency of the electrolyzer is a source of uncertainty with a high impact on the final result. Higher efficiencies result in lower LCOH and vice versa, where the function follows a quadradic pattern. The replacement cost of the electrolyzer stack has a higher impact on the LCOH than the investment cost of the geological storage. Both, however, has a less significant impact on the system cost than the electrolyzer efficiency.

5. Discussion

The freedom of choice between RE sources and the grid in Scenario 1 led to the sole use of electricity from the grid due to low spot prices in the relevant pricing zone, likely caused by high hydro power penetration and low consumption in this zone [54]. The constant availability of electricity from the grid in Scenario 1, compared to the intermittent availability of RE in the other scenarios, allows for a better utilization of the electrolyzer's capacity. Since the electrolyzer and the electricity supply are the system's main cost factors, this has a high impact on the LCOH. In Scenario 2, the power limitation of the grid connection required additional RE capacity to be built. The electrolyzer, however, is dimensioned in a way that not much RE needs to be curtailed but electricity from the grid is purchased to supplement the hydrogen production in times of low wind speeds.

In contrast, in Scenario 3 to 6, where the utilization of the grid is prohibited and electricity generation is dependent on the intermittently available RE sources, higher capacities of both the electrolyzer and hydrogen storage are required to efficiently utilize RE when it is available and store hydrogen for times of low wind speeds. However, the higher hydrogen storage capacity also leads to higher hydrogen losses and decreased system efficiency, resulting in higher LCOH.

The utilization of tanks to store hydrogen in Scenario 5 and 6 increase the LCOH significantly, compared to the use of a geological storage type, as in Scenario 3 and 4. This leads to further oversizing of the electrolyzer capacity to decrease the storage requirement. Although the transport distance to the final consumption unit is marginal in Scenario 5 and 6, the decrease in transport cost cannot compensate for the increase in the storage cost.

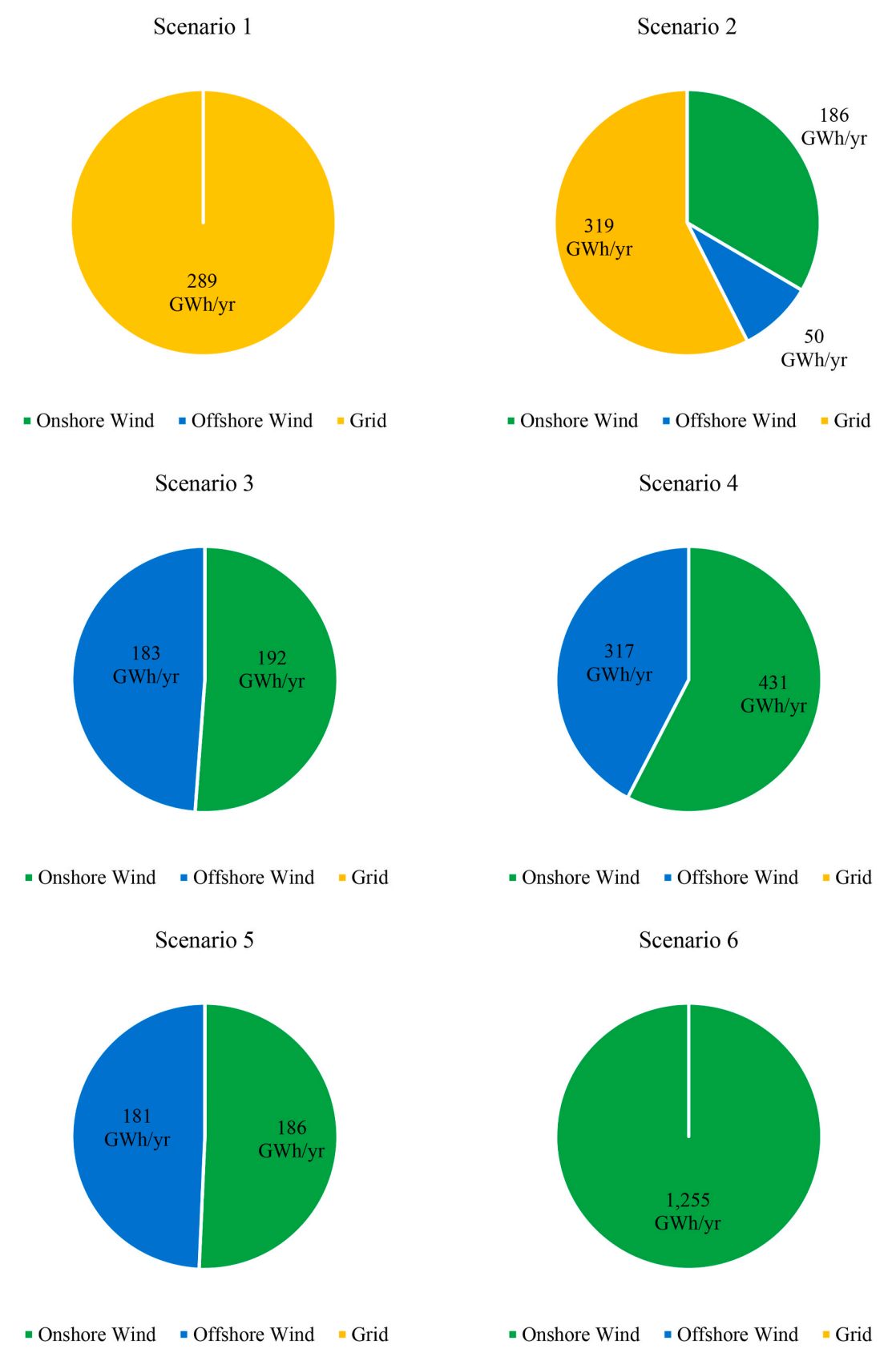
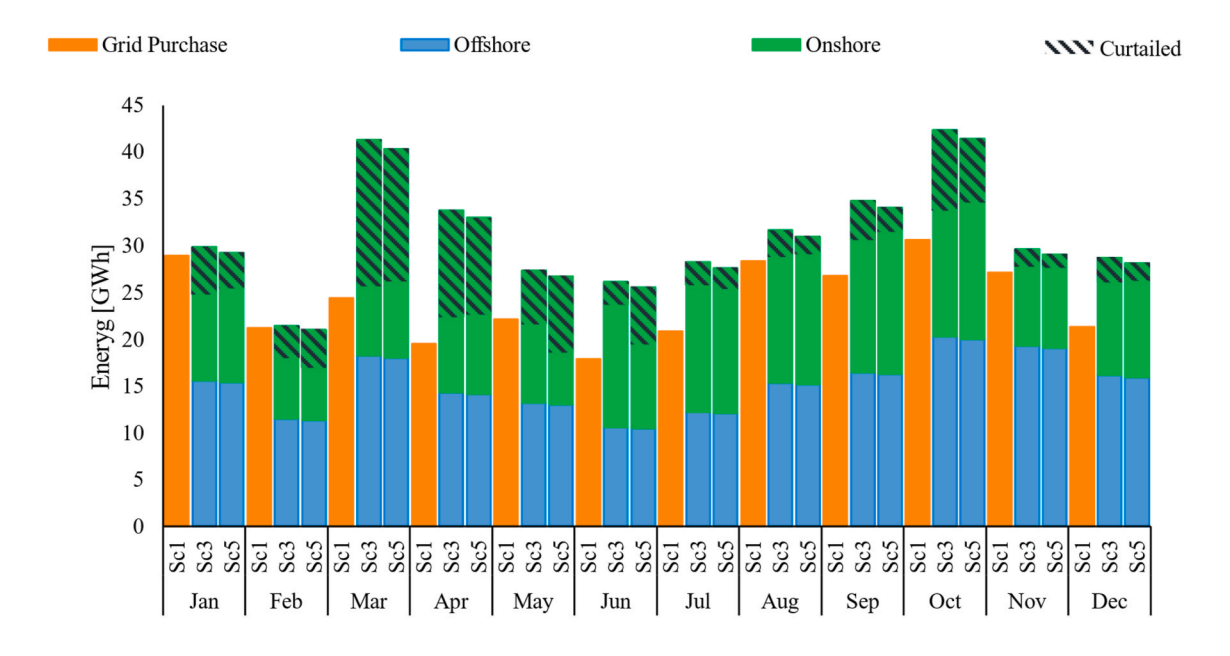


Fig. 14. Yearly electricity generation and purchase for all Scenarios.



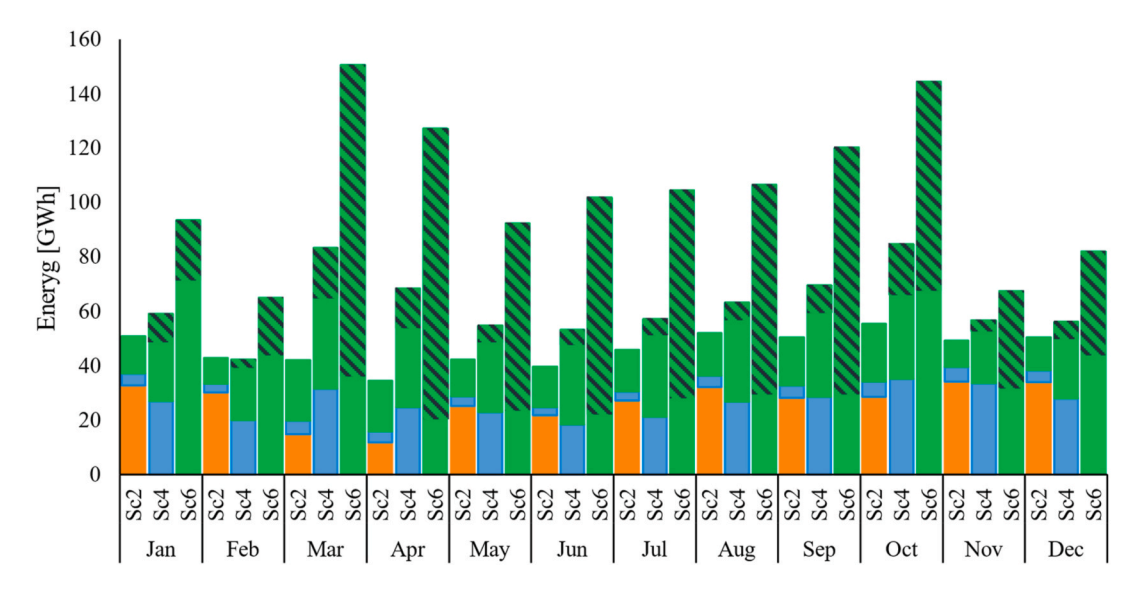


Fig. 15. Electricity Generation and Utilization in each scenario per month for Demand Case 1 (upper) and Demand Case 2 (lower).

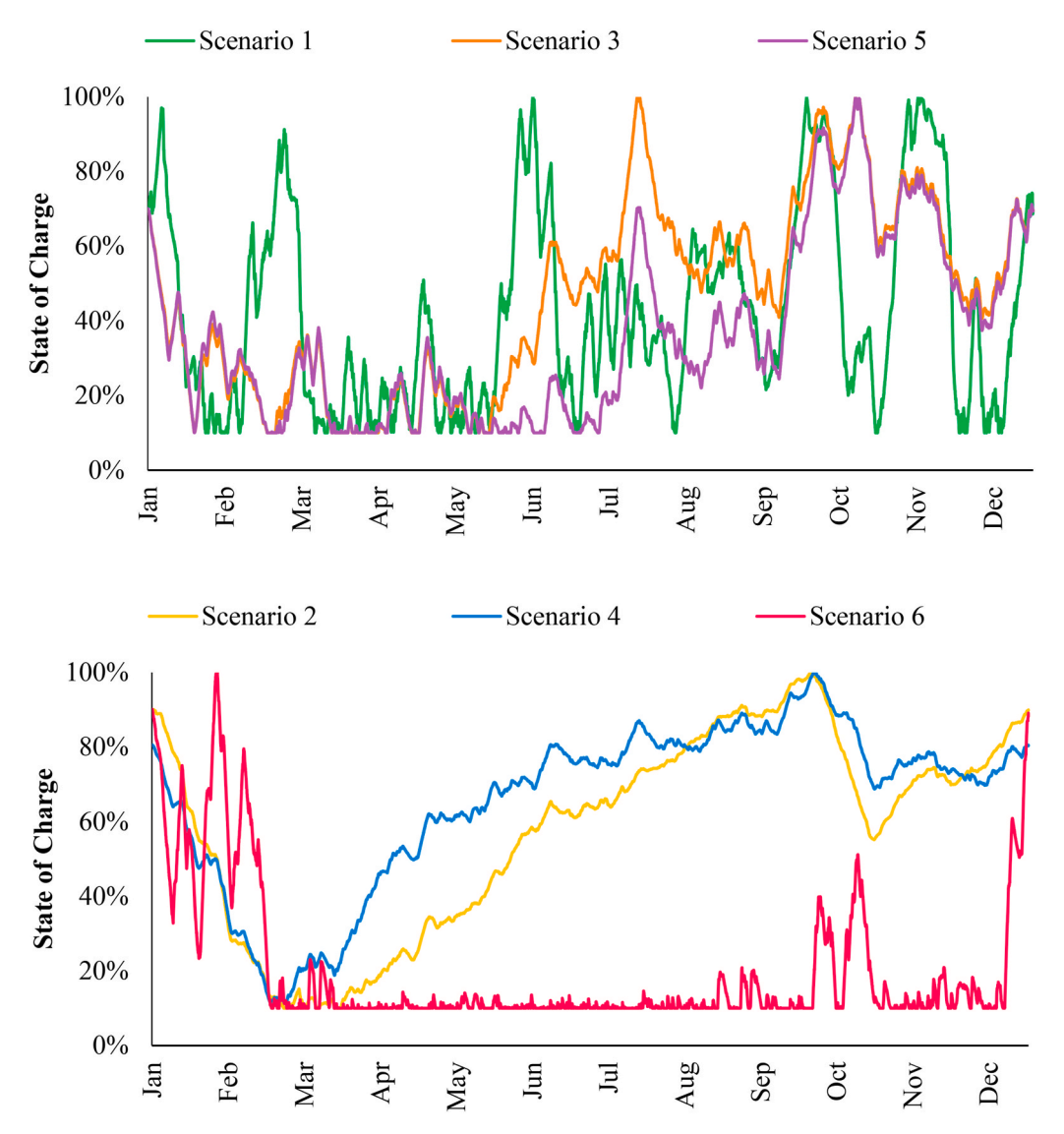


Fig. 16. Hydrogen Storage - State of Charge throughout the year for Demand Case 1 (upper) and Demand Case 2 (lower).

Table 14
Levelized Cost of Hydrogen (LCOH) per supply chain stage for each scenario in [EUR/kg_{H2}].

Scenario	Electricity Purchase and Generation	Electrolysis	Compression	Storage	Transport	Total
Sc1	2.3	2.5	0.02	0.08	0.2	5.2
Sc2	3.5	2.6	0.02	0.61	0.13	6.8
Sc3	8.6	4.3	0.03	0.3	0.2	13.5
Sc4	6.5	3.7	0.03	0.91	0.11	11.3
Sc5	8.5	4.8	0.06	3.8	0.11	17.2
Sc6	8.5	8.8	0.11	3.6	0	21.1

Comparing the results for all scenarios with Demand Case 1 to those considering Demand Case 2, the substantial impact of the demand pattern on the supply chain layout, dispatch, and cost can be seen, while all other boundary conditions are kept unchanged. Demand Case 2, with a higher peak consumption and higher volatility requires disproportionately higher capacities for RE generation, hydrogen production, and storage. Since hydrogen is stored on a seasonal basis, large amounts of hydrogen are stored over a long period, leading to significant losses and thus, lower system efficiency.

In none of the presented scenarios, a battery storage is part of the optimum layout, due to its high investment cost and limited storage capacity. The model shows that the storage of hydrogen in its gaseous

form is a more feasible option to store energy over a longer period. However, in the model, the sale of electricity to the spot market is not considered and therefore, the results neglects revenue streams from battery storage when using it for energy arbitrage and ancillary services.

The cost impact of the hydrogen compressors is minimal (2%) and thus, not discussed further in this research. Based on investigating other scenarios, which are not presented in this research, the choice of transport type affects the system layout and dispatch only marginally, as no transport time requirement or logistic schedule is considered. Therefore, the transport type only affects the total system cost, thereby rendering further discussion on this aspect not useful. Noteworthy is the ascendency of the pipeline as the preferred transport modality across all

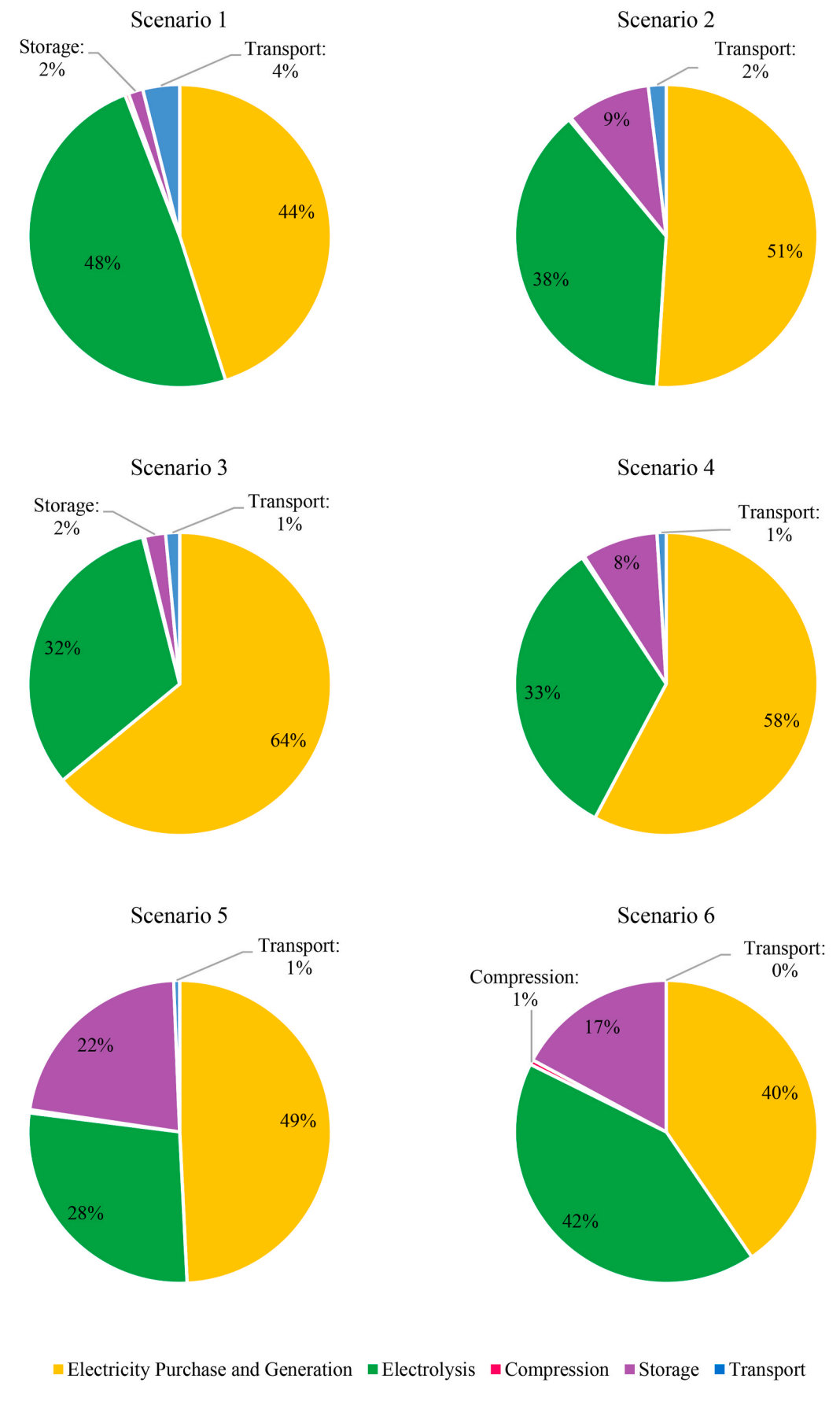


Fig. 17. Share per supply chain stage on the total system cost for all scenarios.

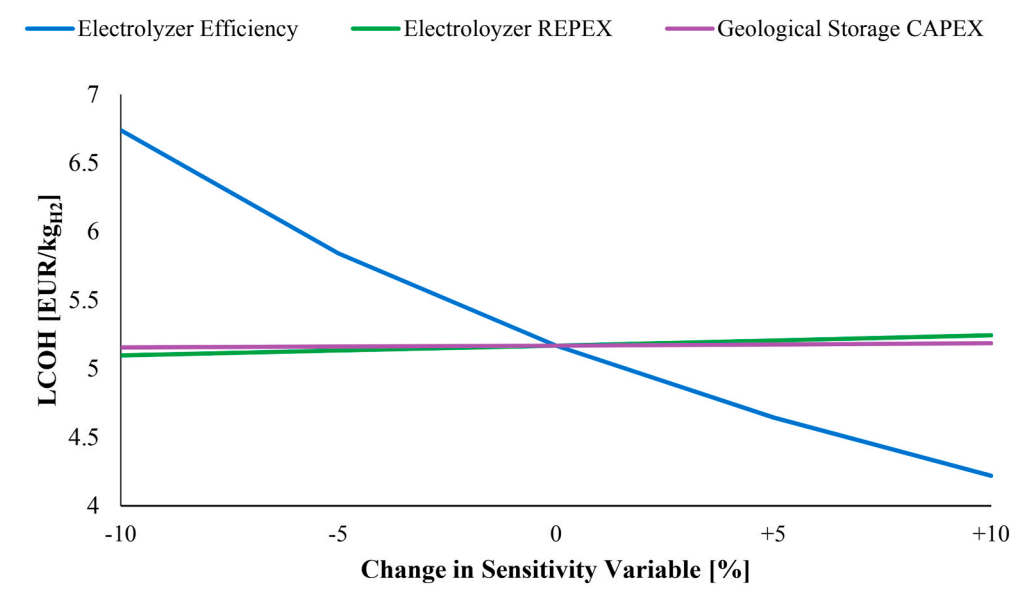


Fig. 18. Result of the sensitivity analysis.

scenarios. This can be attributed to three main reasons: (1) the amount of hydrogen; (2) the assumed distance from the storage to the demand; (3) the utilization of the transport flexible linepack. The flexible linepack, serving as a short-term buffer, demonstrates minimal impact relative to the total storage capacity, and its impact on the pipeline's life span is disregarded.

In consideration of geographical factors, PV emerges as a non-competitive option in comparison to wind power in northern Sweden in connection with increased hydrogen demand during winter and is consequently excluded from the optimal supply chain design. The model considers that the unutilized electricity is to be curtailed as it does not factor in the sale of RE to the grid. Future work can consider additional revenue streams from the sale of RE, excess hydrogen, oxygen, and heat as mitigation strategies for system cost. However, to maximize the revenue from the sale of RE on the electricity spot market against the production of hydrogen, the consideration of a hydrogen market is necessary, which again requires the estimation of prices for hydrogen.

One of the main limitations of the model is the hourly time step of the optimization, which poses challenges in accurately capturing the fluctuations inherent in RE availability and hydrogen demand. Another limitation of the model is that it assumes perfect foresight as all input data is known during the optimization process, thereby neglecting the uncertainty of predictions. This oversimplification may compromise the robustness of the dispatch schedule, potentially impacting system efficiency.

6. Conclusion

This study developed a MILP-based model to optimize the layout and dispatch schedule of a low-carbon hydrogen supply chain, which was applied to a case study in the Swedish industry. Based on our analysis, we draw the following key concluding remarks:

Optimal Configuration: the least-cost supply chain comprises a PEM electrolyzer, a Lined Rock Cavern for storage, and a pipeline for transportation, resulting in an LCOH of 5.2 EUR/kgH2.

Demand Scenario Influence: for scenarios with seasonally occurring peaks (Demand Case 2), LCOH increases to 6.8 EUR/kgH2, requiring additional RE generation.

Cost Drivers: primary cost drivers are electricity generation and purchase expenses, along with electrolyzer installation and operation costs. Geological hydrogen storage has a lower impact on costs compared to pressurized tanks.

Case Dependency: optimal layout and operation are case-

dependent. The study emphasizes the importance of a less volatile electricity availability and hydrogen demand, which can lead to decreased system costs due to smaller capacity requirements and an increased ability to utilize existing capacity more efficiently throughout the supply chain. Furthermore, not only the volatility but also the peak demand increases system cost due to decreased capacity utilization throughout the whole supply chain.

Complexity of the Supply Chain: the study underscores the interconnected nature of the hydrogen supply chain. Smoothing demand variation and aligning electricity availability with hydrogen demand are crucial for minimizing system costs.

In summary, the study emphasizes the nuanced considerations necessary for optimizing a low-carbon hydrogen supply chain, shedding light on the intricate balance required between various factors that influence system costs. To further improve the developed model, future research can expand upon the findings and investigate the impact of additional revenue streams, such as the sale of RE to the grid, and the consideration of a dynamic hydrogen market. This will provide a better understanding of the hydrogen supply chain's complexity and help identify the optimal design and operation for a wider range of cases.

CRediT authorship contribution statement

Jan L. Dautel: Conceptualization, Data curation, Formal analysis, Investigation, Methodology, Software, Validation, Visualization, Writing – original draft. **Jagruti Thakur:** Conceptualization, Formal analysis, Investigation, Methodology, Project administration, Resources, Supervision, Writing – review & editing. **Ahmed M. Elberry:** Investigation, Methodology, Supervision, Validation, Writing – review & editing, Conceptualization.

Declaration of competing interest

The authors declare that they have no known competing financial interests or personal relationships that could have appeared to influence the work reported in this paper.

Acknowledgement

This work has been supported by WSP Sverige AB, specifically the department for Energy Strategic Advisory, who provided insights, data, and support for the case study.

Appendix A. Parameter Definition

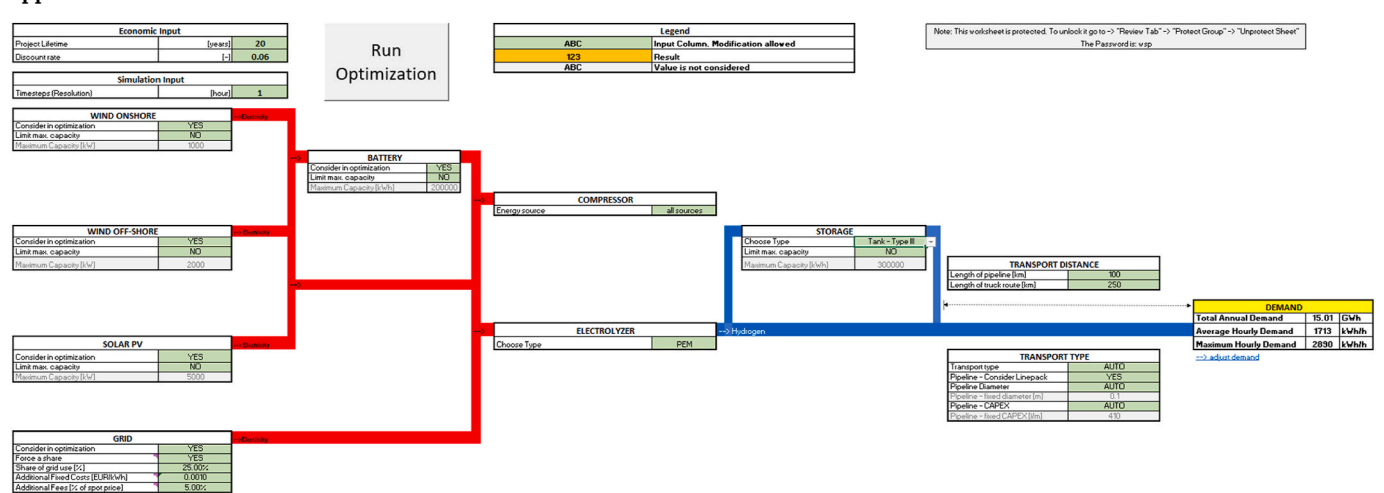


Fig. A1. Screenshot from the SYSTEM-Sheet in the EXCEL Input-File

Off-Shore Wind						
	Unit Default Source Overwrite (Considered	
Economic Parameters						
Initial Investment Costs	[€/kW]		IRENA, n.c		2802.8	
Replacement Costs (2030)	[€/kW]	2314	Ram, M. e		2314	
OPEX as fraction of CAPEX	[-]		Ram, M. e		0.035	
OPEX	[€/kW/yr]	98.098			98.098	
Lifetime of the component	[years]	25	Ram, M. e		25	
	System parai	meters				
System efficiency*	[-]		assumption		0.9	
*Accounts for additional losses	in cables, transformers	etc.				
	Location para	meters				
Surface Roughness of Terrain	[m]	0.0006	Golbazi, N		0.0006	
Roughness for a smooth sea						
	Turbine para	meters				
Default values based on	Gamesa G128-5.0MW		Bauer, L.,			
Hub Height	[m]	1	40		140	
Power Curve	Wind Speed		Pow	er Output		
	[m/s]			[kW]		
	Default	Default		Overwrite	Considered	
	0	0			0	
	1	0			0	
	2	0			0	
	3	59			59	
	4	195			195	
	5	420			420	
	6	786			786	
	7	1296			1296	
	8	1943			1943	
	9	2699			2699	
	10	3487			3487	

Economic Po [€/kW] [€/kW]	777.04 435	s IRENA, n.o		Considered
[€/kW] [€/kW]	777.04 435	IRENA, n.o		
[€/kW] [€/kW]	777.04 435	IRENA, n.o		
[€/kW]	435			
		D 11 -		777.04
[-]		Ram, M. e		435
	1.50%	Ram, M. e		0.015
[€/kW/yr]	11.6556			11.6556
[years]	30	Ram, M. e		30
System po	rameter			
		assumption		0.9
		=Latitude		65.58
		assumption		180
	CET			CET
Location Po	rameters	5		
[deg]	65.58	Luleå		65.58
[deg]	22.16	Luleå		22.16
[m]	0.05	Anjum, L.,		0.05
cables, trans	sformers	etc.		
	[-] [deg] [deg] Location Po [deg] [deg]	[deg] 65.58 [deg] 180 CET Location Parameters [deg] 65.58 [deg] 22.16 [m] 0.05	[-] 90.00% assumption [deg] 65.58 =Latitude [deg] 180 assumption CET Location Parameters [deg] 65.58 Luleå [deg] 22.16 Luleå	[-] 90.00% assumption [deg] 55.58 -Latitude [deg] 180 assumption CET Location Parameters [deg] 65.58 Luleå [deg] 22.16 Luleå [m] 0.05 Anjum, L.,

Fig. A2. Screenshot from the Electricity Generation Sheet in the EXCEL Input-File

Table A1Input Parameter Values – Electricity generation and Electrolyzer

Technology	Parameter	Unit	Value	Reference
Onshore Wind Power	CAPEX	[EUR/kW]	1188	[55]
	OPEX	[EUR/kW]	924	[56]
	REPEX	[% of CAPEX]	2.5%	[56]
	Lifetime	[yr]	25	[56]
	Turbine Type	<u> </u>	Alstrom ECO 122/2700	[57]
Offshore Wind Power	CAPEX	[EUR/kW]	2803	[55]
	OPEX	[EUR/kW]	2314	[56]
	REPEX	[% of CAPEX]	3.5%	[56]

(continued on next page)

Table A1 (continued)

Technology	Parameter	Unit	Value	Reference
	Lifetime	[yr]	25	[56]
	Turbine Type	[-]	Gamesa G128-5.0 MW	[58]
Solar PV	CAPEX	[EUR/kW]	777	[55]
	REPEX	[EUR/kW]	435	[56]
	OPEX	[% of CAPEX]	1.5%	[56]
	Lifetime	[yr]	30	[56]
	PV-Tilt angle	[deg]	Equal to the latitude	
	PV-Azimuth	[deg]	180	
Battery Storage	CAPEX	[EUR/kW]	381	[59]
-	OPEX	[% of CAPEX]	250	[59]
	REPEX	[% of CAPEX]	2.8%	[59]
	Lifetime	[yr]	10	[59]
	Cycle Efficiency	[-]	85%	[60]
	C-Rating	[-]	1	assumption
	Minimum SOC	[-]	10%	assumption
	Maximum SOC	[-]	90%	[61]
	Initial SOC	[-]	20%	assumption
Electricity Grid	Spot Price (SE1, 2021)	[EUR/MWh]	[-]	[47]
•	G^{\max}	50 000	[kW]	assumption
Electrolyzer	CAPEX	[EUR/kW _e]	1491	[62]
	REPEX	[EUR/kWe]	895	[62]
	OPEX	[% of CAPEX]	1.5%	[4]
	Stack Lifetime	[h]	70 000	[63]
	Degradation Limit	[-]	10%	[64]
	Electrolyzer Efficiency (LHV)	[-]	50.1%	[63]
	Output Pressure	[bar]	30	[63]

Table A2Input Parameter Values – Hydrogen Storage, Compression, and Transport

Technology	Parameter	Unit	Value	Reference
Hydrogen Storage	CAPEX	[EUR/kWh]	1.43	[43]
Lined Rock Cavern	REPEX	[EUR/kWh]	1.43	[43]
	OPEX	[% of CAPEX]	5%	[65]
	Lifetime	[yr]	40	[66]
	Operating Pressure	[bar]	110	[67]
	Loss per day	[% of stored energy]	0.0095	[68]
	Minimum SOC during operation	[-]	10%	
	Initial SOC	[-]	90%	
Hydrogen Storage Depleted Oil Reservoir	CAPEX	[EUR/kWh]	0.02	[43]
	REPEX	[EUR/kWh]	0.02	[43]
	OPEX	[% of CAPEX]	5 %	[65]
	Lifetime	[yr]	40	[66]
	Operating Pressure	[bar]	150	[67]
	Loss per day	[% of stored energy]	0.0095	[68]
	Minimum SOC during operation	[-]	10 %	
	Initial SOC	[-]	90 %	
Hydrogen Storage – Tank Type I	CAPEX	[EUR/kWh]	23	[69]
	REPEX	[EUR/kWh]	23	[69]
	OPEX	[% of CAPEX]	2.5 %	[66]
	Lifetime	[yr]	20	[26]
	Operating Pressure	[bar]	250	[42]
	Loss per day	[% of stored energy]	0 %	[26]
	Minimum SOC during operation	[-]	10 %	assumpti
	Initial SOC	[-]	90 %	assumpti
Hydrogen Storage – Tank Type III	CAPEX	[EUR/kWh]	46	[69]
	REPEX	[EUR/kWh]	46	[69]
	OPEX	[% of CAPEX]	2.5 %	[66]
	Lifetime	[yr]	20	[26]
	Operating Pressure	[bar]	325	[42]
	Loss per day	[% of stored energy]	0 %	[26]
	Minimum SOC during operation	[-]	10 %	assumpti
	Initial SOC	[-]	90 %	assumpti

(continued on next page)

Table A2 (continued)

Technology	Parameter	Unit	Value	Reference
Compressor	CAPEX	[EUR/kW]	1255	[70]
	REPEX	[EUR/kW]	1255	[70]
	OPEX	[% of CAPEX]	6%	[69]
	Lifetime	[yr]	15	[40]
	Isentropic Efficiency	[-]	80%	[40]
	Electric Engine Efficiency	[-]	95%	[40]
	Mass losses	[-]	0.5%	[71]
Transport - Truck	Hourly Truck Costs	[EUR/h]	133.3	[52]
•	Average Speed	[km/h]	50	[72]
	Loading and Unloading Requirement	[h]	2	[11]
	Truck Pressure	[bar]	350	[52]
	Truck Capacity	[kg/truck]	345	[52]
Transport - Pipeline	OPEX	[% of CAPEX]	2%	[73]
	Lifetime	[yr]	40	[26]
	Required Output Pressure	[bar]	30	[11]
	Operational Pressure	[bar]	70	[11]
	Flow Velocity	[m/s]	15	[44]
	Maximum Distance between Booster Stations	[km]	100	[74]
	Initial SOC of the Linepack	[-]	20%	

Appendix B. Additional Mathematic Documentation

The concept of Levelized Cost of Hydrogen

To optimize the hydrogen supply chain, the model utilizes the concept of Levelized Cost of Hydrogen (LCOH) as a performance metric. LCOH is defined as the total discounted cost of hydrogen production over the economic lifespan of the project [30]. It provides a comprehensive measure, considering both the costs and performance aspects critical for the assessment and enhancement of the hydrogen supply chain.

$$LCOH = \frac{NPC}{NPV_{H2}} = \frac{\sum_{n=0}^{N} \frac{CAPEX_n + REPEX_n + OPEX_n - SALVAGE_n}{(1+d)^n}}{\sum_{n=0}^{N} \frac{Q_{H2,n}}{1+d^n}}$$
 B1

Where;

NPC:Net Present Cost throughout the project economic span [EUR]

NPV_{H2}:Total discounted sum of hydrogen produced over the project economic span [kg]

 $Q_{H2,n}$:Amount of hydrogen produced in year n [kg]

N:Length of the project period [years]

d:Discount rate

 $CAPEX_n$: Capital Expenses in year n = 0 [EUR]

REPEX_n:Replacement cost required in the year of replacement.

OPEX_n:Operational Expense of the component per year

 $SALVAGE_n$: Remaining value of an asset at the end of the project (n = N), considering a linear depreciation over components' life span.

Roughness-dependent geographical interpolation of surface wind speed averages

$$\frac{c_{\rm h}^{\rm hub}}{c_{\rm h}^{\rm measured}} = \frac{ln^{\frac{z_{\rm anemometer}}{z_0}}}{ln^{\frac{z_{\rm hub}}{z_0}}}$$
B2

Where,

 c_h^{hub} - Hourly wind speed at hub height

 z_{hub} - Height of the anemometer $\,$

 $c_h^{measured}$ - Measured wind speed at height z_0 .

Power Curves for the considered onshore and offshore wind turbines

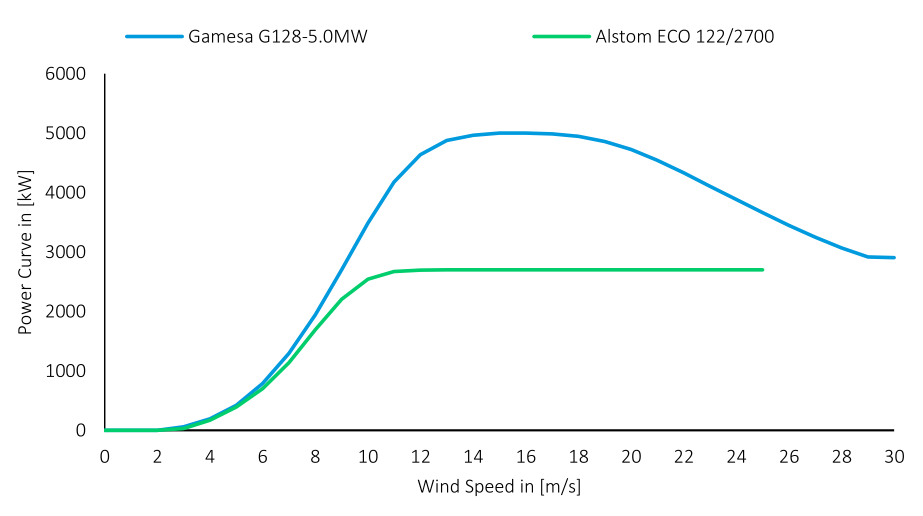


Fig. B1. Power curves for the two considered wind turbine types

Solar PV – Coefficients for Crystalline Silican PV cells

Table B1 Values of coefficients used in (4 for Crystalline Silicon PV cells [38].

Coefficient	Value
k_1	-0.017237
k_2	-0.040465
k_3	-0.004702
k_4	0.000149
k_5	0.000170
k_6	0.000005

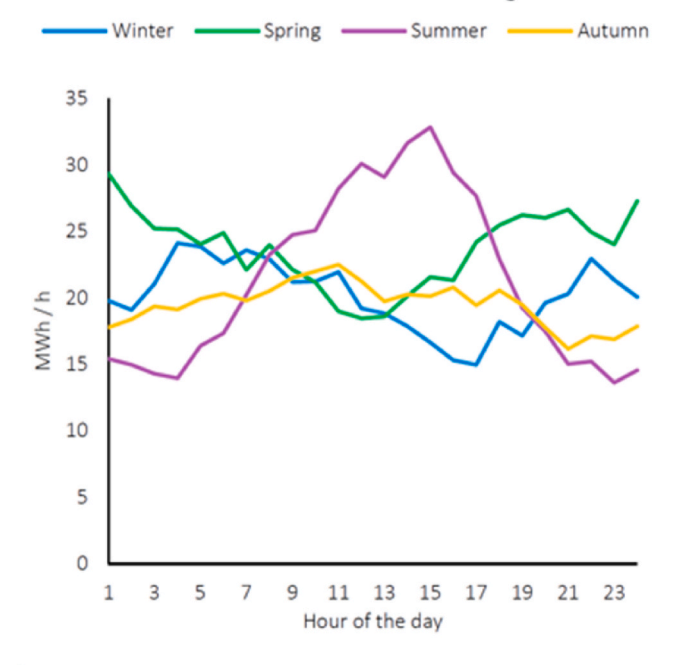
Appendix C. Results

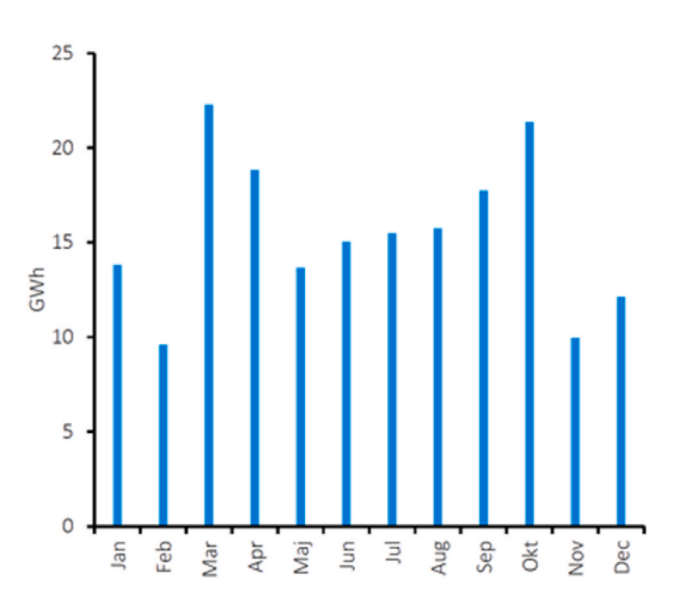
Seasonal Daily Pattern

Monthly Accumulation

Wind Power Production - Daily Pattern

Wind Power Production - Accumulated





Chronologic Operation

Renewable Energy Availability

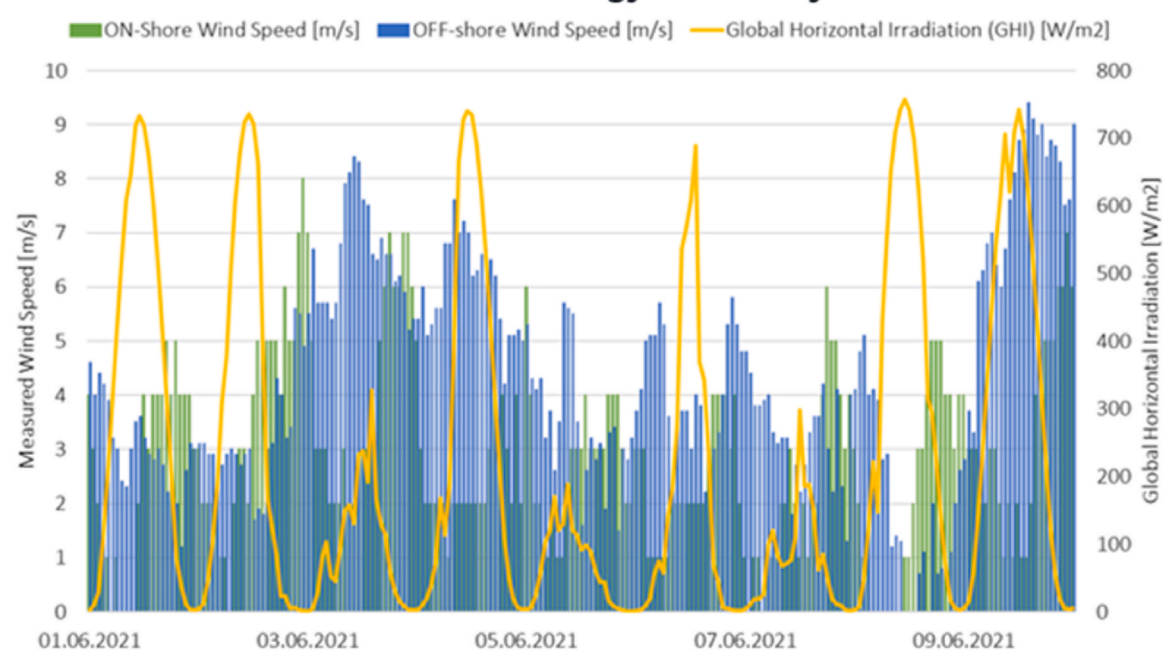


Fig. C1. Example of Visualization of Patterns in the EXCEL Result-File

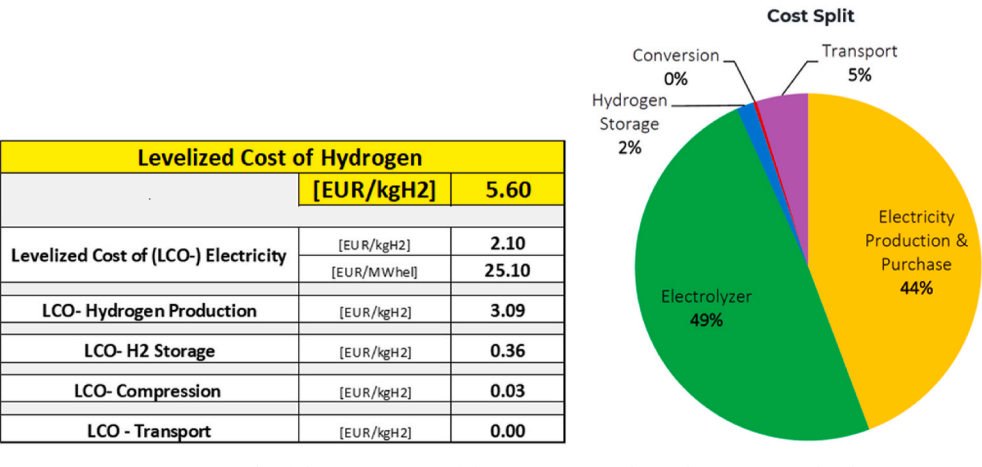
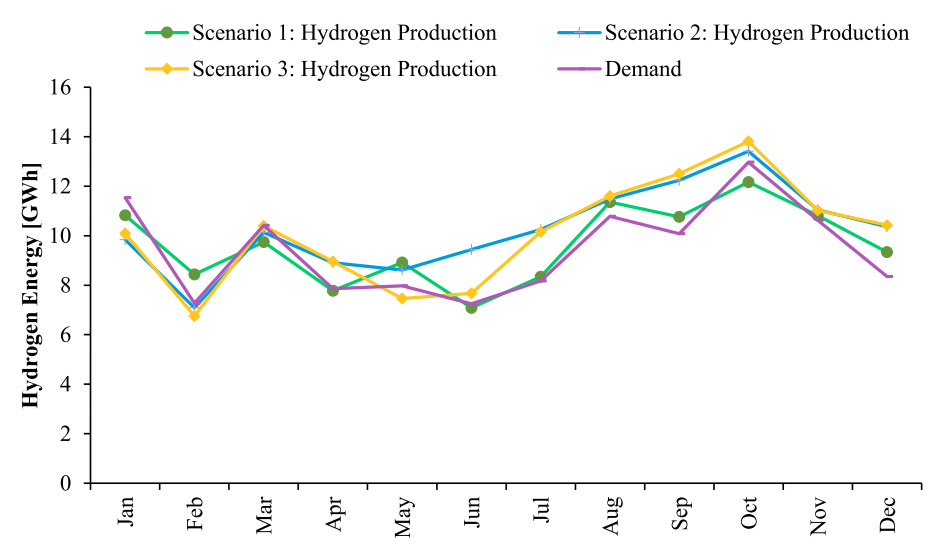


Fig. C2. Example of the Presentation of the Economic Results in the EXCEL Result File



 $\textbf{Fig. C3.} \ \ \textbf{Hydrogen Demand Case 1} \ \ \textbf{and Production for Scenario 1, 3, and 5}$

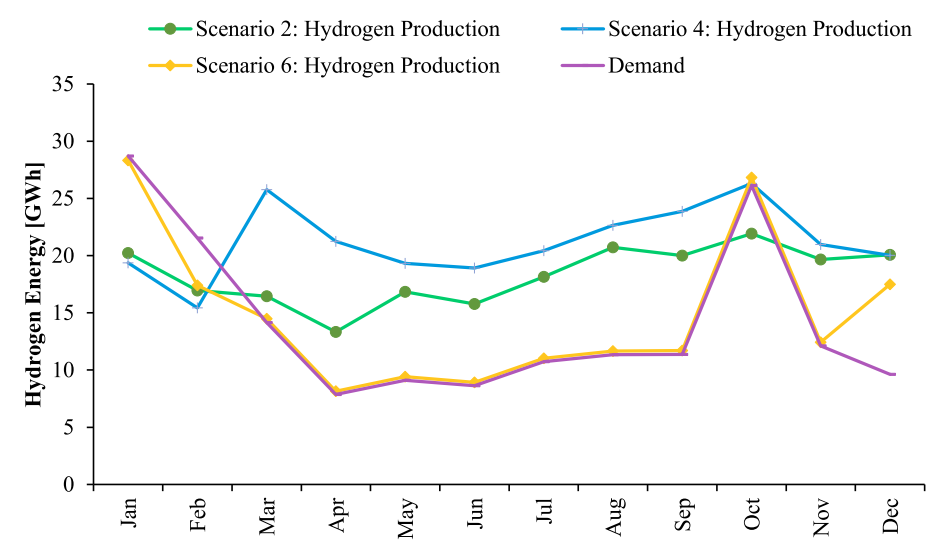


Fig. C4. Hydrogen Demand Case 2 and Production for Scenario 2, 4, and 6

References

- [1] Vogler J. Changing conceptions of climate and energy security in Europe. Environ Polit Jul. 2013;22(4):627–45. https://doi.org/10.1080/09644016.2013.806634.
- [2] European Comission. The European green deal [Online]. Available: https://eur-lex.europa.eu/legal-content/EN/TXT/?uri=COM%3A2019%3A640%3AFIN. [Accessed 15 September 2022].
- [3] European Comission. REPowerEU plan [Online]. Available: https://eur-lex.europa.eu/legal-content/EN/TXT/?uri=COM%3A2022%3A230%3AFIN&qid=1653033742483. [Accessed 15 September 2022].
- [4] IEA. The future of hydrogen. Sep. 2022. p. 203.
- [5] Kayfeci M, Keçebaş A, Bayat M. Chapter 3 hydrogen production. In: Calise F, D'Accadia MD, Santarelli M, Lanzini A, Ferrero D, editors. Solar hydrogen production. Academic Press; 2019. p. 45–83. https://doi.org/10.1016/B978-0-12-814853-2.00003-5.
- [6] Janssen JLLCC, Weeda M, Detz RJ, van der Zwaan B. Country-specific cost projections for renewable hydrogen production through off-grid electricity systems. Appl Energy Mar. 2022;309:118398. https://doi.org/10.1016/j. apenergy.2021.118398.
- [7] Chi J, Yu H. Water electrolysis based on renewable energy for hydrogen production. Chin J Catal Mar. 2018;39(3):390–4. https://doi.org/10.1016/S1872-2067(17)62949-8.
- [8] Demir ME, Dincer I. Cost assessment and evaluation of various hydrogen delivery scenarios. Int J Hydrogen Energy May 2018;43(22):10420–30. https://doi.org/ 10.1016/j.iihydene.2017.08.002.
- [9] Elberry AM, Thakur J, Santasalo-Aarnio A, Larmi M. Large-scale compressed hydrogen storage as part of renewable electricity storage systems. Int J Hydrogen Energy Apr. 2021;46(29):15671–90. https://doi.org/10.1016/j. iihydene.2021.02.080.
- [10] Mintz M, et al. Hydrogen delivery scenario analysis model for hydrogen distribution options. Transport Res Rec Jan. 2006;1983(1):114–20. https://doi. org/10.1177/0361198106198300116.
- [11] Yang G, Jiang Y, You S. Planning and operation of a hydrogen supply chain network based on the off-grid wind-hydrogen coupling system. Int J Hydrogen Energy Aug. 2020;45(41):20721–39. https://doi.org/10.1016/j. iihydene 2020 05 207
- [12] Tashie-Lewis BC, Nnabuife SG. Hydrogen production, distribution, storage and power conversion in a hydrogen economy - a technology review. Chem Eng J Adv Nov. 2021;8:100172. https://doi.org/10.1016/j.ceja.2021.100172.
- [13] Elberry AM, Thakur J, Veysey J. Seasonal hydrogen storage for sustainable renewable energy integration in the electricity sector: a case study of Finland. J Energy Storage Dec. 2021;44:103474. https://doi.org/10.1016/j. est 2021 103474.
- [14] Mintz M, et al. Hydrogen delivery scenario analysis model for hydrogen distribution options. Transport Res Rec Jan. 2006;1983(1):114–20. https://doi. org/10.1177/0361198106198300116.
- [15] Li L, Feng L, Manier H, Manier M-A. Life cycle optimization for hydrogen supply chain network design. Int J Hydrogen Energy Jan. 2024;52:491–520. https://doi. org/10.1016/i.iihydene.2022.03.219.
- [16] Li L, Manier H, Manier M-A. Integrated optimization model for hydrogen supply chain network design and hydrogen fueling station planning. Comput Chem Eng Mar. 2020;134:106683. https://doi.org/10.1016/j.compchemeng.2019.106683.
- [17] De-León Almaraz S, Azzaro-Pantel C, Montastruc L, Pibouleau L, Senties OB. Assessment of mono and multi-objective optimization to design a hydrogen supply chain. Int J Hydrogen Energy Nov. 2013;38(33):14121–45. https://doi.org/ 10.1016/j.ijhydene.2013.07.059.
- [18] Husarek D, Schmugge J, Niessen S. Hydrogen supply chain scenarios for the decarbonisation of a German multi-modal energy system. Int J Hydrogen Energy Nov. 2021;46(76):38008–25. https://doi.org/10.1016/j.ijhydene.2021.09.041.
- [19] Nunes P, Oliveira F, Hamacher S, Almansoori A. Design of a hydrogen supply chain with uncertainty. Int J Hydrogen Energy Dec. 2015;40(46):16408–18. https://doi. org/10.1016/j.ijhydene.2015.10.015.
- [20] Erdoğan A, Güler MG. Optimization and analysis of a hydrogen supply chain in terms of cost, CO2 emissions, and risk: the case of Turkey. Int J Hydrogen Energy Jul. 2023;48(60):22752–65. https://doi.org/10.1016/j.ijhydene.2023.04.300.
- [21] Brändle G, Schönfisch M, Schulte S. Estimating long-term global supply costs for low-carbon hydrogen. Appl Energy Nov. 2021;302:117481. https://doi.org/ 10.1016/j.apenergy.2021.117481.
- [22] Riera JA, Lima RM, Knio OM. A review of hydrogen production and supply chain modeling and optimization. Int J Hydrogen Energy Apr. 2023;48(37):13731–55. https://doi.org/10.1016/j.ijhydene.2022.12.242.
- [23] De-León Almaraz S, Azzaro-Pantel C, Montastruc L, Domenech S. Hydrogen supply chain optimization for deployment scenarios in the Midi-Pyrénées region, France. Int J Hydrogen Energy Aug. 2014;39(23):11831–45. https://doi.org/10.1016/j. iihydene.2014.05.165.
- [24] Gallardo F, Monforti Ferrario A, Lamagna M, Bocci E, Astiaso Garcia D, Baeza-Jeria TE. A Techno-Economic Analysis of solar hydrogen production by electrolysis in the north of Chile and the case of exportation from Atacama Desert to Japan. Int J Hydrogen Energy 2021;46(26):13709–28.
- [25] Seo S-K, Yun D-Y, Lee C-J. Design and optimization of a hydrogen supply chain using a centralized storage model. Appl Energy Mar. 2020;262:114452. https://doi.org/10.1016/j.apenergy.2019.114452.
- [26] Reuß M, Grube T, Robinius M, Preuster P, Wasserscheid P, Stolten D. Seasonal storage and alternative carriers: a flexible hydrogen supply chain model. Appl Energy Aug. 2017;200:290–302. https://doi.org/10.1016/j. apenergy.2017.05.050.

- [27] Chen Q, Gu Y, Tang Z, Wang D, Wu Q. Optimal design and techno-economic assessment of low-carbon hydrogen supply pathways for a refueling station located in Shanghai. Energy Dec. 2021;237:121584. https://doi.org/10.1016/j. energy.2021.121584.
- [28] Bynum ML, et al. Pyomo-optimization modeling in python. Third., vol. 67. Springer Science & Business Media; 2021.
- [29] Jin L, Tang Q, Zhang C, Shao X, Tian G. More MILP models for integrated process planning and scheduling. Int J Prod Res Jul. 2016;54(14):4387–402. https://doi. org/10.1080/00207543.2016.1140917.
- [30] Lazart. Lazard's Levelized cost of hydrogen analysis [Online]. Available: https://www.lazard.com/media/451779/lazards-levelized-cost-of-hydrogen-analysis-vf.pdf. [Accessed 15 September 2022].
- [31] Wieringa J. Roughness-dependent geographical interpolation of surface wind speed averages. Q J R Meteorol Soc 1986;112(473):867–89. https://doi.org/ 10.1002/gi.49711247316.
- [32] Physics of wind turbines | energy fundamentals [Online]. Available: https://home. uni-leipzig.de/energy/energy-fundamentals/15.htm. [Accessed 20 December 2022]
- [33] What is global horizontal irradiance? :: solar online tools FAQ :: support :: 3TIER [Online]. Available: https://www.3tier.com/en/support/solar-prospecting-tools/what-global-horizontal-irradiance-solar-prospecting/. [Accessed 20 December 2022].
- [34] Holmgren WF, Hansen CW, Mikofski MA. Pvlib python: a python package for modeling solar energy systems. JOSS Sep. 2018;3(29):884. https://doi.org/ 10.21105/josc.00884
- [35] Erbs DG, Klein SA, Duffie JA. Estimation of the diffuse radiation fraction for hourly, daily and monthly-average global radiation. Sol Energy Jan. 1982;28(4):293–302. https://doi.org/10.1016/0038-092X(82)90302-4.
- [36] Crystalline Silicon Photovoltaics Research," Energy Gov. Accessed: December. 20, 2022. [Online]. Available: https://www.energy.gov/eere/solar/crystalline-silicon-photovoltaics-research.
- [37] Huld T, Amillo A. Estimating PV module performance over large geographical regions: the role of irradiance, air temperature, wind speed and solar spectrum. Energies Jun. 2015;8(6):5159–81. https://doi.org/10.3390/en8065159.
- [38] Huld T, et al. A power-rating model for crystalline silicon PV modules. Sol Energy Mater Sol Cell Dec. 2011;95(12):3359–69. https://doi.org/10.1016/j. solmat 2011.07.026
- [39] Saur G. Wind-to-hydrogen project: electrolyzer capital cost study. Dec. 2008. https://doi.org/10.2172/944892. NREL/TP-550-44103, 944892.
- [40] Khan MA, Young C, Mackinnon C, Layzell DB. The techno-economics of hydrogen compression. Technical Briefs Canada: Transition Accelerator 2021;1(1):1e36.
- [41] Moran MJ, Shapiro HN, Boettner DD, Bailey MB. Fundamentals of engineering thermodynamics. John Wiley & Sons; 2010.
- [42] Langmi HW, Engelbrecht N, Modisha PM, Bessarabov D. Chapter 13 hydrogen storage. In: Smolinka T, Garche J, editors. Electrochemical power sources: fundamentals, systems, and applications. Elsevier; 2022. p. 455–86. https://doi. org/10.1016/B978-0-12-819424-9.00006-9.
- [43] HyUnder. Overview on all known underground storage technologies for hydrogen [Online]. Available: http://hyunder.eu/wp-content/uploads/2016/01/D3.1_Over view-of-all-known-underground-storage-technologies.pdf. [Accessed 5 January 2023].
- [44] Baufumé S, et al. GIS-based scenario calculations for a nationwide German hydrogen pipeline infrastructure. Int J Hydrogen Energy Apr. 2013;38(10): 3813–29. https://doi.org/10.1016/j.ijhydene.2012.12.147.
- [45] Quarton CJ, Samsatli S. Should we inject hydrogen into gas grids? Practicalities and whole-system value chain optimisation. Appl Energy Oct. 2020;275:115172. https://doi.org/10.1016/j.apenergy.2020.115172.
- [46] Rohrreibung [Online]. Available: https://www.maschinenbau-wissen.de/skript3/fluidtechnik/hydraulik/198-rohrreibung. [Accessed 2 November 2022].
- [47] Nordpool. Day ahead electricity sport market [Online]. Available: https://www.nordpoolgroup.com/en/Market-data1/Dayahead/Area-Prices/ALL1/Hourly/. [Accessed 12 December 2022].
- [48] SMHI. SMHI Luleå-Kallax Flygplats [Online]. Available: https://www.smhi.se/data/meteorologi/ladda-ner-meteorologiska-observationer/#param=wind,stations=core,stationid=162860. [Accessed 9 December 2022].
- [49] SMHI. SMHI Rödkallen A [Online]. Available: https://www.smhi.se/data/met eorologi/ladda-ner-meteorologiska-observationer/#param=wind,stations=core, stationid=162790. [Accessed 9 December 2022].
- [50] SMHI, "SMHI Luleå Sol Air Temperature." Accessed: October. 18, 2022. [Online]. Available: https://www.smhi.se/data/meteorologi/ladda-ner-meteorologiska-observationer/#param=globalIrradians,stations=all,stationid=162015
- [51] P. Zhang, "Hydrogen storage in lined rock caverns Luleå University of Technology," Luleå University of Technology. Accessed: January. 10, 2023. [Online]. Available: https://www.ltu.se/centres/CH2ESS/Forskning/Distribution-lagring/Vatgaslager-i-inkladda-bergrum-1.220296?l=en.
- [52] Ulleberg Ø, Hancke R. Techno-economic calculations of small-scale hydrogen supply systems for zero emission transport in Norway. Int J Hydrogen Energy Jan. 2020;45(2):1201–11. https://doi.org/10.1016/j.ijhydene.2019.05.170.
- [53] Öhman A. Green hydrogen production at Igelsta CHP plant: a techno-economic assessment conducted at Söderenergi AB [Online]. Available: http://urn.kb. se/resolve?urn=urn:nbn:se:kth:diva-299434. [Accessed 4 January 2023].
- [54] Wråke M, Kofoed-Wiuff A, Svensson VD, Hethey J. Impact on electricity prices of added generation in southern Sweden [Online]. Available: https://energiforsk.se /media/30978/energiforsk-rapport-2022-845-impact-on-electricity-prices-ofadded-generation-in-southern-sweden.pdf; Feb. 2022.

- [55] IRENA. Renewable power generation costs in 2020 [Online]. Available: https://www.irena.org/publications/2021/Jun/Renewable-Power-Costs-in-2020. [Accessed 8 December 2022].
- [56] Ram M, Child M, Aghahosseini A, Bogdanov D, Lohrmann A. A comparative analysis of electricity generation costs from renewable, fossil fuel and nuclear sources in G20 countries for the period 2015-2030. J Clean Prod Oct. 2018;199: 687-704. https://doi.org/10.1016/j.jclepro.2018.07.159.
- [57] Bauer L. Alstom ECO 122/2700 2,70 MW wind turbine [Online]. Available: https://en.wind-turbine-models.com/turbines/629-alstom-eco-122-2700. [Accessed 15 October 2022].
- [58] Bauer L. Gamesa G128-5.0MW 5,00 MW wind turbine [Online]. Available: https://en.wind-turbine-models.com/turbines/767-gamesa-g128-5.0mw. [Accessed 9 December 2022].
- [59] NREL, "Utility-scale battery storage," Tableau Software. Accessed: December. 12, 2022. [Online]. Available: https://public.tableau.com/views/2021CMTS/TechSummary?:embed=y&Technology=Utility-Scale%20Battery%20Storage&:embed=y&:showVizHome=n&:bootstrapWhenNotified=y&:apiID=handler0.
- [60] Rancilio G, Merlo M, Lucas A, Kotsakis E, Delfanti M. BESS modeling: investigating the role of auxiliary system consumption in efficiency derating. In: 2020 international symposium on power electronics, electrical drives, automation and motion (SPEEDAM); Jun. 2020. p. 189–94. https://doi.org/10.1109/ SPEEDAM48782.2020.9161875.
- [61] Steckel T, Kendall A, Ambrose H. Applying levelized cost of storage methodology to utility-scale second-life lithium-ion battery energy storage systems. Appl Energy Oct. 2021;300:117309. https://doi.org/10.1016/j.apenergy.2021.117309.
- [62] Böhm H, Goers S, Zauner A. Estimating future costs of power-to-gas a component-based approach for technological learning. Int J Hydrogen Energy Nov. 2019;44 (59):30789–805. https://doi.org/10.1016/j.ijhydene.2019.09.230.
- [63] IRENA. Green hydrogen cost reduction [Online]. Available: https://www.irena.or g/publications/2020/Dec/Green-hydrogen-cost-reduction. [Accessed 4 January 2023].
- [64] Bertuccioli L, Chan A, Hart D, Lehner F, Madden B, Standen E. Development of water electrolysis in the European Union. 2014.

- [65] Smith N, Ceri V. Geological database report. Hystories 2022 [Online]. Available: https://hystories.eu/wp-content/uploads/2022/05/Hystories_D1.2-0-Geological-database-report.pdf. [Accessed 1 May 2023].
- [66] Frank E, Gorre J, Ruoss F, Friedl MJ. Calculation and analysis of efficiencies and annual performances of Power-to-Gas systems. Appl Energy May 2018;218: 217–31. https://doi.org/10.1016/j.apenergy.2018.02.105.
- [67] Gas Infrastructure Europe. Picturing the value of underground gas storage to the European hydrogen system - gas Infrastructure EuropeGas Infrastructure Europe [Online]. Available: https://www.gie.eu/gie-presents-new-study-picturing-thevalue-of-underground-gas-storage-to-the-european-hydrogen-system/. [Accessed 5 January 2023].
- [68] Lord AS, Kobos PH, Borns DJ. Geologic storage of hydrogen: scaling up to meet city transportation demands. Int J Hydrogen Energy Sep. 2014;39(28):15570–82. https://doi.org/10.1016/j.ijhydene.2014.07.121.
- [69] U.S. Department of Energy, "DOE Technical Targets for Hydrogen Delivery," Energy Gov. Accessed: January. 4, 2023. [Online]. Available: https://www.energy.gov/eere/fuelcells/doe-technical-targets-hydrogen-delivery.
- [70] Lahnaoui A, Wulf C, Heinrichs H, Dalmazzone D. Optimizing hydrogen transportation system for mobility via compressed hydrogen trucks. Int J Hydrogen Energy Jul. 2019;44(35):19302–12. https://doi.org/10.1016/j. ijhydene.2018.10.234.
- [71] Graf M. Costs and energy efficiency of long-distance hydrogen transport options. 2021
- [72] Svenson G, Gjeld D. The impact of road geometry and surface roughness on driving speed for Swedish logging trucks [Online]. Available: https://hvttforum.org/wp-c ontent/uploads/2019/11/Svenson-Impact-of-road-geometry-and-surface-roughn ess-on-driving-speed-for-Swedish-logging-trucks.pdf. [Accessed 9 December 2022].
- [73] van Gerwen R, Eijgelaar M, Bosma T. Hydrogen in the electricity value chain DNV [Online]. Available: https://www.dnv.com/Publications/hydrogen-in-the-ele ctricity-value-chain-225850. [Accessed 9 December 2022].
- [74] Nelik L. "Pumps and systems in transcontinental energy transfer," pumps and systems magazine [Online]. Available: https://www.pumpsandsystems.com/p umps-and-systems-transcontinental-energy-transfer. [Accessed 9 December 2022].